A

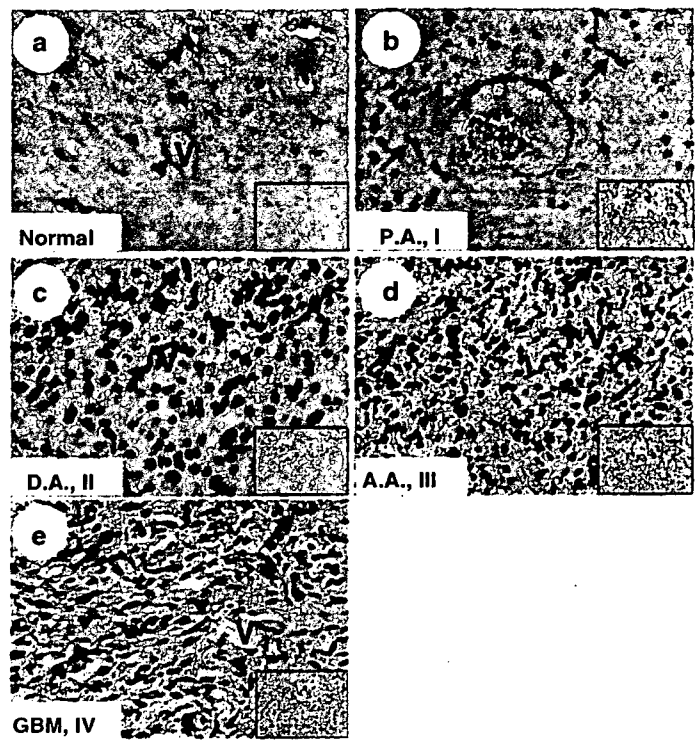

B **NRP-1 Expression Correlates with Human Glioma Progression**

WHO grade	n	Histology	n	Score -	±	1+	2+	3+	Kruskal-Wallis test* with Scheffe's post-hoc test
Normal	4	Normal	4	4	0	0	0	0	Normal+I
I	4	Pilocytic astrocytoma	4	0	4	0	0	0	Normal+I
II	24	Oligodendroglioma	13	2	4	5	2	0	II
		Diffuse astrocytoma	10	0	0	5	5	0	II
		Oligoastrocytoma	1	0	0	1	0	0	II
III	21	Anaplastic astrocytoma	13	0	1	7	5	0	III+IV
		Anaplastic oligodendroglioma	7	0	0	3	3	1	III+IV
		Anaplastic oligoastocytoma	1	0	0	0	1	0	III+IV
IV	43	Glioblastoma multiforme	43	0	3	16	18	6	III+IV

Normal+I vs II: $p < 0.01$; II vs III+IV: $p < 0.05$; Normal+I vs III+IV: $p < 0.01$

*Kruskal-Wallis test between Normal+Grade I vs Grade II vs Grade III+IV showed significant difference with $p < 0.00001$. Differences between each group were then examined by Scheffe's post-hoc test and each p-value were indicated in the table.

n, number of specimens. Score, intensity of IHC staining in the clinical specimens by an ant-NRP1-antibody and is defined as described in the Materials and Method section.

Figure 1 NRP1 expression correlates with human glioma progression. (**A**) IHC of paraffin sections of normal human brain (panel a), P.A. (WHO grade I, panel b), diffuse astrocytoma (D.A., grade II, panel c), anaplastic astrocytoma (A.A., grade III, panel d) and GBM (grade IV, panel e) tissue. Insets in panels a–e are the isotype-matched IgG control staining of identical areas. Arrows indicate neurons (a) or tumor cells (b to e) that are positive for NRP1. Arrowheads indicate endothelial cells in tumor-associated vessels that express NRP1. Results are representative of three independent experiments. Original magnification: ×400. (**B**) Statistical analyses. A total of 92 individual primary tumor specimens (WHO grade I–IV) and four normal human brain biopsies were analysed.

U87MG, LacZ and NRP1 cells secreted VEGF (30 ± 3.6 ng/ml/10^6 cells), FGF-2 (14 ± 2.1 pg/ml/10^6 cells) and HGF/SF (400 ± 45 pg/ml/10^6 cells) into serum-free medium at similar levels. A neutralizing anti-HGF/SF antibody abolished the effect of NRP1-enhanced U87MG cell survival, whereas neutralizing anti-FGF-2 and anti-VEGF antibodies had little or no effect on cell survival of U87MG and NRP1 cells (Figure 4B).

To investigate whether the HGF/SF/c-Met signaling pathway mediates NRP1 stimulation of glioma cells, we examined the expression and tyrosine phosphorylation

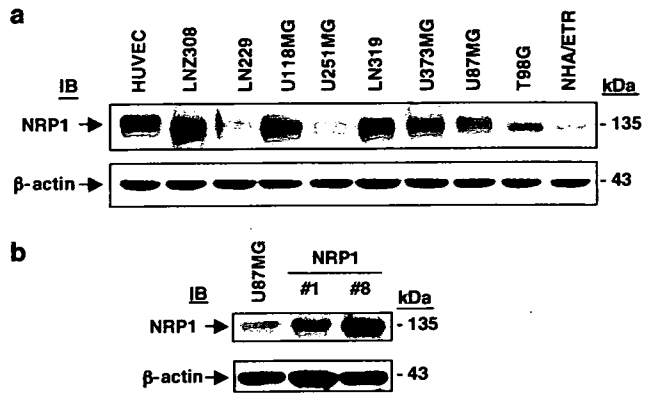

Figure 2 Overexpression of NRP1 in U87MG glioma cells. IB analyses of HUVEC, NHA/ETR and various glioma cell lines (**a**) or U87MG and NRP1-no. 1 and NRP1-no. 8 cells (**b**) using a polyclonal anti-NRP1 antibody (C-18). β-Actin was used as a loading control. Similar results were also obtained using a polyclonal anti-NRP1 antibody (NP1ECD1A). Results are representative of three independent experiments.

of c-Met in U87MG and NRP1 cells in the absence or presence of the HGF/SF neutralizing antibody. As shown in Figure 4C, in the absence of serum, expression of endogenous c-Met was not enhanced by NRP1 overexpression, but tyrosine phosphorylation of c-Met was stimulated in NRP1 but not U87MG or LacZ cells. When the HGF/SF neutralizing antibody was included in the cell culture, the NRP1-induced phosphorylation of c-Met was diminished. As U87MG, LacZ and NRP1 cells secrete low levels of endogenous HGF/SF in the serum-free CM (400 ± 45 pg/ml/10^6 cells) and no inhibitory effect of the neutralizing anti-HGF/SF on U87MG parental cell survival (Figure 4B) was seen, we reasoned that the HGF/SF/c-Met autocrine signaling pathway was not activated due to low levels of the endogenous HGF/SF in U87MG or LacZ cells. Furthermore, NRP1 overexpression in U87MG cells potentiated HGF/SF/c-Met autocrine signaling by activating a downstream target, Bad, an antiapoptotic molecule (Abounader and Laterra, 2005) (Figure 4C). Phosphorylation of Bad at Ser-112 was induced by NRP1 overexpression, but only a slight enhancement occurred on the constitutively phosphorylated Ser-136 of Bad. Additionally, a 4-day culture in serum-free medium did not alter the expression levels of NRP1 in U87MG, LacZ or NRP1-expressing cells (Figure 4D).

Although U87MG cells are deficient in plexin A1 and VEGFR-2, Sema 3A, a cognate ligand for NRP1, is expressed in U87MG cells (Rieger *et al*., 2003). Thus, we tested a specific knockdown of Sema 3A by siRNA to examine the effects of endogenous Sema 3A on NRP1-enhanced U87MG cell growth. As shown in Figure 4E, endogenous c-Met (panel a) and Sema 3A (panel b) were considerably suppressed compared with the control siRNA-transfected cells. Reduced expression of c-Met, but not Sema 3A, in NRP1 cells significantly abolished the NRP1-enhanced U87MG cell survival (Figure 4F).

NRP1 potentiates glioma cell proliferation in response to exogenous HGF/SF

We assessed whether NRP1 overexpression could potentiate stimulation of glioma cell proliferation by exogenous HGF/SF using a BrdUrd incorporation assay. As shown in Figure 5A, in the absence of recombinant human (rh) HGF/SF, the basal level of BrdUrd incorporation in NRP1-no. 1 and -no. 8 cells was similar to that in U87MG and LacZ cells. When cells were treated with 5 or 10 ng/ml of rhHGF/SF, a significant increase in BrdUrd incorporation was found in NRP1-no. 1 and -no. 8 cells compared with U87MG and LacZ cells, whereas stimulation by 25 ng/ml rhHGF/SF markedly enhanced BrdUrd incorporation in U87MG and LacZ cells. Further increases of rhHGF/SF (50 or 75 ng/ml) had no further augmentation of BrdUrd incorporation in U87MG, LacZ and NRP1 cells. Also, NRP1-potentiated cell proliferation was proportional to the level of exogenous NRP1 expression in the glioma cells when comparing the BrdUrd incorporation level in NRP1-no. 8 cells (higher level of exogenous NRP1) to NRP1-no. 1 cells (lower level of NRP1 expression, Figure 2b).

Next, we assessed the activation of c-Met and two of its downstream effectors, ERK and Bad. As shown in Figure 5B, when cells were treated with 10 ng/ml rhHGF/SF for 20 or 40 min, phosphorylation of ERK1/2 and Bad at Ser-112 was evident in NRP1-expressing cells but not in LacZ cells. Moreover, treatment with 25 μmol/l U0126, a specific inhibitor for ERK, inhibited HGF/SF-stimulated phosphorylation of ERK and Bad as well as BrdUrd incorporation in NRP1 cells but not in LacZ cells (Figure 5Ca and b). To a similar extent, suppression of Bad protein expression in these cells by a specific siRNA (Figure 5Da) also significantly attenuated HGF/SF-stimulated BrdUrd incorporation in NRP1 cells but had no effect on LacZ cells or untreated cells (Figure 5Db).

To further confirm the critical role of NRP1 expression on potentiation of HGF/SF/c-Met signaling, we determined the effects of endogenous NRP1 on cell growth in LNZ-308 glioma cells, as LNZ-308 cells express endogenous NRP1 at high levels (Figure 2a) and no endogenous HGF/SF protein was detected by ELISA in serum-free CM (data not shown). As shown in Figure 6a, three individual siRNAs for NRP1 (N1, N2 and N3) suppressed endogenous NRP1 protein at various levels in LNZ-308 cells, whereas a pool of these three siRNAs for NRP1 (N1:N2:N3 = 1:1:1) considerably suppressed endogenous NRP1 protein. When control siRNA-transfected LNZ-308 cells were stimulated with rhHGF/SF, BrdUrd incorporation increased by 1.6-fold in response to 10 ng/ml of rhHGF/SF and reached a peak when 20 ng/ml HGF/SF was used (Figure 6b). Stimulation by HGF/SF on LNZ-308 cells at higher concentrations (60 and 80 ng/ml) had no further effect (Figure 6b). Importantly, when endogenous NRP1 expression was inhibited using siRNA, HGF/SF-stimulated BrdUrd incorporation at low concentrations (10 and 20 ng/ml) was significantly attenuated.

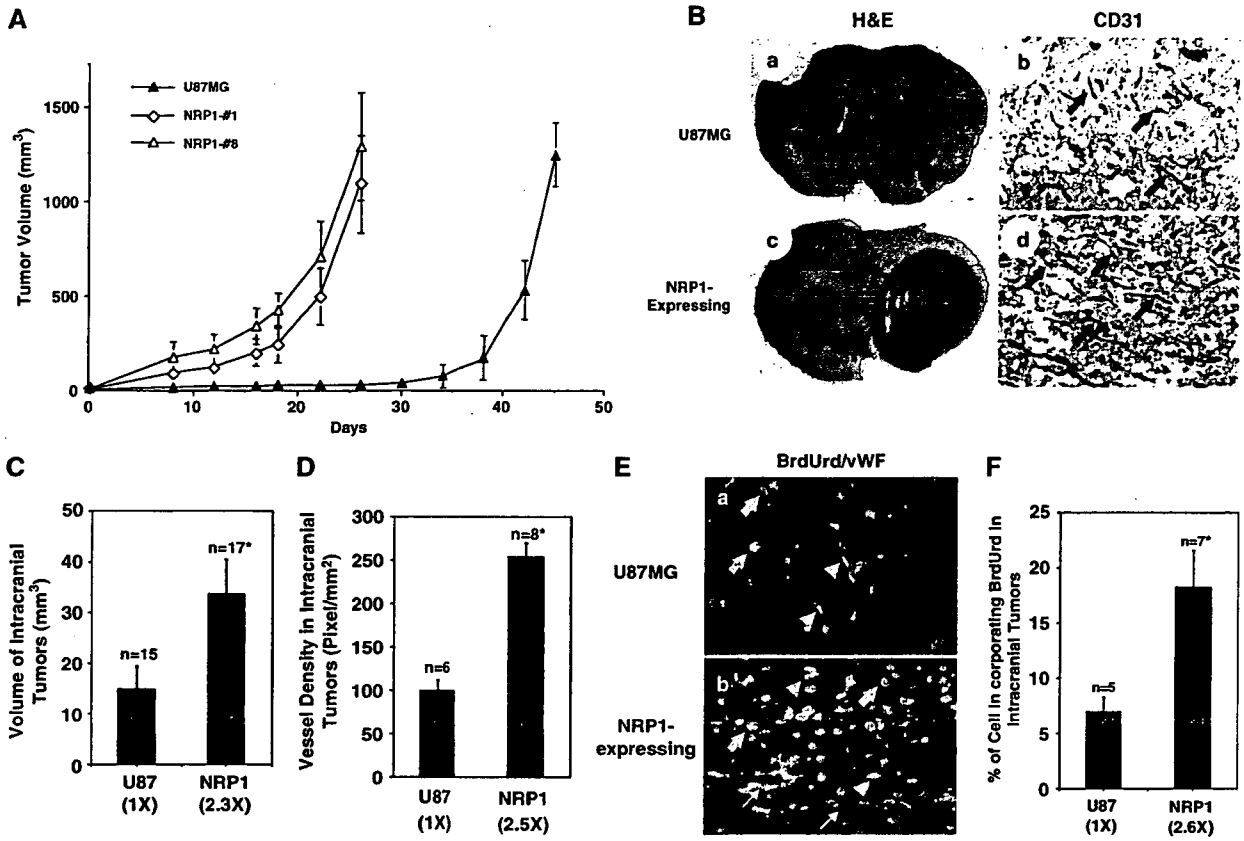

Figure 3 Overexpression of NRP1 in U87MG cells promotes tumor growth and angiogenesis. (A) Growth kinetics of U87MG or NRP1 tumors at subcutaneous sites. Tumor volume was estimated (volume = $(a^2 \times b)/2$, $a < b$) using a caliper at the indicated times. Data are shown as mean ± s.d. (B) Tumorigenicity and angiogenesis of U87MG brain tumors. IHC analyses are shown for U87MG (panels a and b) or NRP1 (c and d) gliomas. Panels a and c are brain sections stained with hematoxylin and eosin (H&E). Panels b and d show CD31 staining for tumor vessels. Arrows in a and c, tumor mass. Arrows in b and d, blood vessels. Five to eight individual tumor samples of each group from each *in vivo* experiment were analysed. Original magnification: panels a and c, × 12.5; b and d, × 200. (C) and (D) Quantitative analyses of tumorigenesis and angiogenesis in various intracranial tumors. Data are means ± s.d. Numbers in parentheses, the difference in fold between U87MG and NRP1 gliomas. (E) and (F) Cell proliferation of various intracranial gliomas. (E) IHC staining of U87MG brain tumors with a monoclonal anti-BrdUrd antibody (red) together with a polyclonal anti-vWF antibody (green). Blue arrows, proliferative nuclei in tumor cells. White arrows, proliferative nuclei of blood vessels. Blue arrowheads, vWF staining of vessels. Three to five serial sections from five to seven individual samples of each tumor type were analysed. Original magnification: × 400. (F) Quantitative analyses of cellular BrdUrd incorporation in U87MG and U87MG/NRP1 tumors. Numbers in parentheses, the difference in fold between U87MG/NRP1 and parental U87MG gliomas. Results in (A–E) are representative of three independent experiments.

Next, we examined activation of the HGF/SF/c-Met signaling pathway in various siRNA-transfected LNZ-308 cells in response to HGF/SF stimulation. As shown in Figure 6c, HGF/SF stimulation at 10, 25 and 50 ng/ml induces phosphorylation of c-Met, Erk1/2 and Bad. When NRP1 expression was suppressed using siRNA, the activation by HGF/SF at 10 and 25 ng/ml on c-Met, ERK1/2 and Bad was diminished. No inhibitory effect on HGF/SF stimulation was seen when NRP1 siRNA-transfected LNZ-308 cells were treated with 50 ng/ml HGF/SF.

NRP1 enhances HGF/SF/Met signaling in human glioma

Next, we sought to determine whether activation of c-Met also occurred in NRP1-expressing tumors *in vivo*. We extracted tissue lysates from U87MG and NRP1 tumors and performed IB analysis. As shown in Figure 7a, NRP1 overexpression did not increase c-Met expression in the NRP1 tumors. However, increased phosphorylation of c-Met was detected in the tissue lysates of NRP1 tumors compared with the parental tumors established at subcutaneous and orthotopic sites. Finally, we examined whether increased expression of NRP1 and c-Met phosphorylation correlates with glioma progression in 14 primary human glioma tissue samples by IB analyses. As shown in Figure 7b, c-Met was detected at various levels in all of the glioma tissues, whereas upregulation of NRP1 expression was seen primarily in high-grade tumors (grades III and IV). Importantly, c-Met phosphorylation was also increased in high-grade gliomas, mostly in grade IV GBM specimens, correlating with the expression profile of NRP1 in these clinical samples.

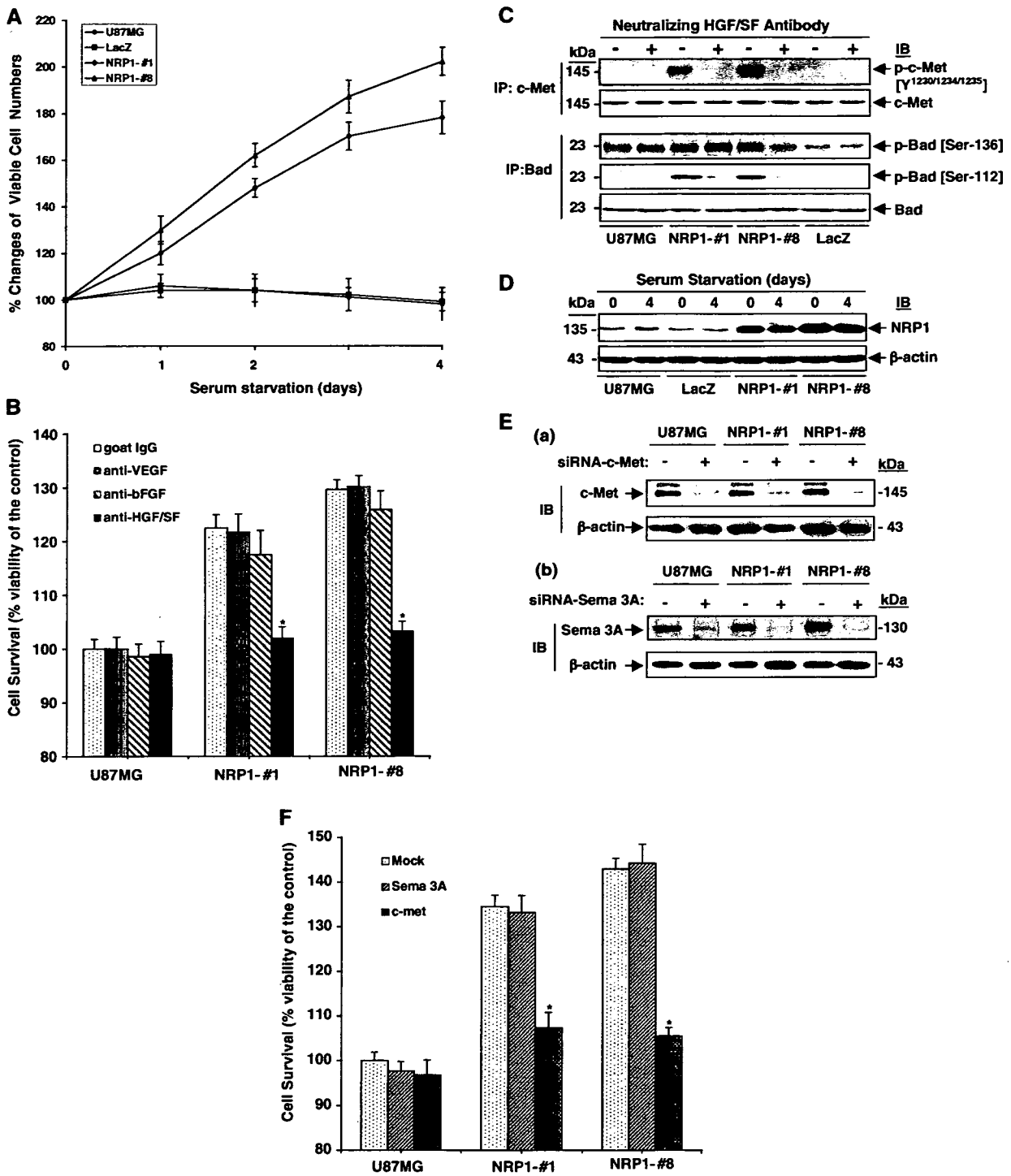

Figure 4 NRP1 promotes survival of U87MG cells by enhancing autocrine HGF/SF/c-Met signaling. (**A**) Overexpression of NRP1 promotes U87MG cell survival. Data of cell survival assays are shown as mean ± s.d. (**B**) Inhibition of HGF/SF, but not FGF-2 or VEGF, suppresses NRP1-promoted U87MG cell survival. Data of cell survival assays are shown as mean ± s.d. (**C**) Inhibition of tumor cell-derived HGF/SF, but not VEGF or FGF-2, suppresses NRP1-potentiated activation of c-Met and Bad. IP and IB analyses of various U87MG cells treated with or without the HGF/SF neutralizing antibody. (**D**) Serum starvation did not alter NRP1 expression in U87MG, LacZ and NRP1 cells. IB analyses of various cell lysates under the same conditions as in (**A**). (**E**) and (**F**) Inhibition of endogenous c-Met but not Sema 3A attenuates NRP1-potentiated U87MG cell viability. (**E**) Suppression of endogenous c-Met and Sema 3A by siRNA. IB analyses of c-Met and Sema 3A proteins in various U87MG cells. (**F**) Cell survival assays of siRNA-transfected U87MG and NRP1 cells. Data are shown as mean ± s.d. In (**B–D**), c-Met, Bad and β-actin were used as loading controls. Results in (**A–F**) are representative of three independent experiments.

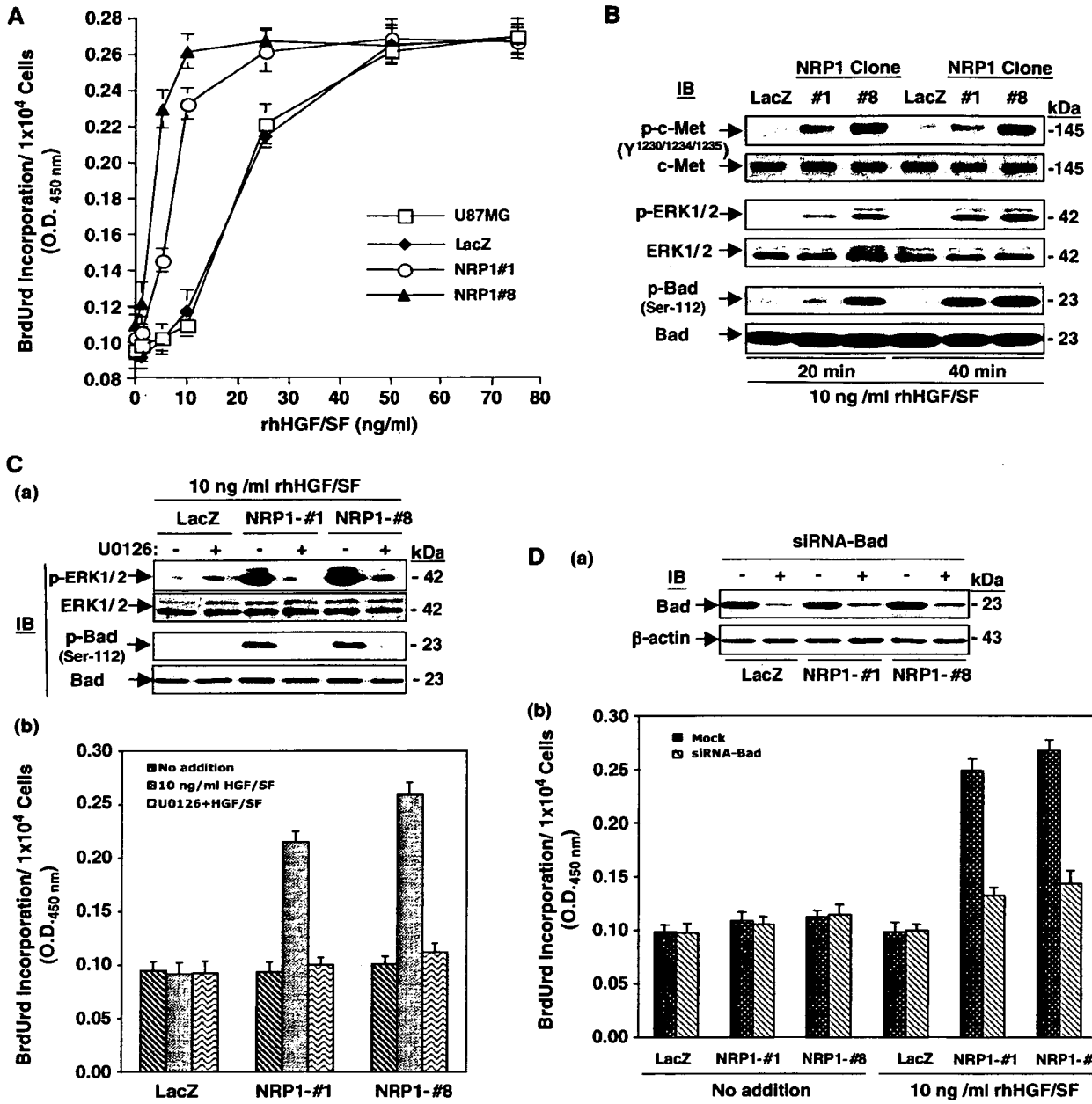

Figure 5 NRP1 expression potentiates HGF/SF stimulation of cell proliferation mediated by c-Met signaling. (**A**) Expression of NRP1 in U87MG cells potentiates cell proliferation in response to a low dose of HGF/SF stimulation. Data of BrdUrd incorporation in U87MG, LacZ, NRP1-no. 1, and NRP1-no. 8 cells are shown as mean±s.d. (**B**) IB analyses of NRP1-potentiated HGF/SF stimulation of phosphorylation on c-Met, ERK1/2 and Bad in various U87MG cells. (**C**) U0126 attenuated NRP1-potentiated HGF/SF stimulation of phosphorylation on ERK1/2 and Bad (panel a, IB analyses) and cell proliferation in various U87MG cells (panel b, BrdUrd incorporation assays; data are shown as mean±s.d.). (**D**) Knockdown of Bad by siRNA (panel a, IB analyses) attenuates NRP1-potentiated HGF/SF stimulation of cell proliferation in various U87MG cells (panel b, data are shown as mean±s.d.). In (**B–D**), c-Met, ERK1/2, Bad and β-actin were used as loading controls. Results in (**A**) to (**D**) are representative of three independent experiments.

Discussion

The role of NRP1 in human tumor progression has been studied in various cancer model systems. Upregulation of NRP1 was found not only in endothelia but also in tumor cells in various types of primary human cancer specimens (Ding *et al.*, 2000; Akagi *et al.*, 2003). Overexpression of NRP1 in tumor cells has been shown to promote tumor growth and angiogenesis in xenograft models and cell survival in cancer cells. In these reports, NRP1 stimulation of tumor progression was primarily attributed to VEGF-dependent pathways (Miao *et al.*, 2000; Bachelder *et al.*, 2003). This study provides new evidence that glioma cell-expressed NRP1 promotes tumor progression through potentiating the HGF/SF/c-Met signaling pathway. We show in primary human

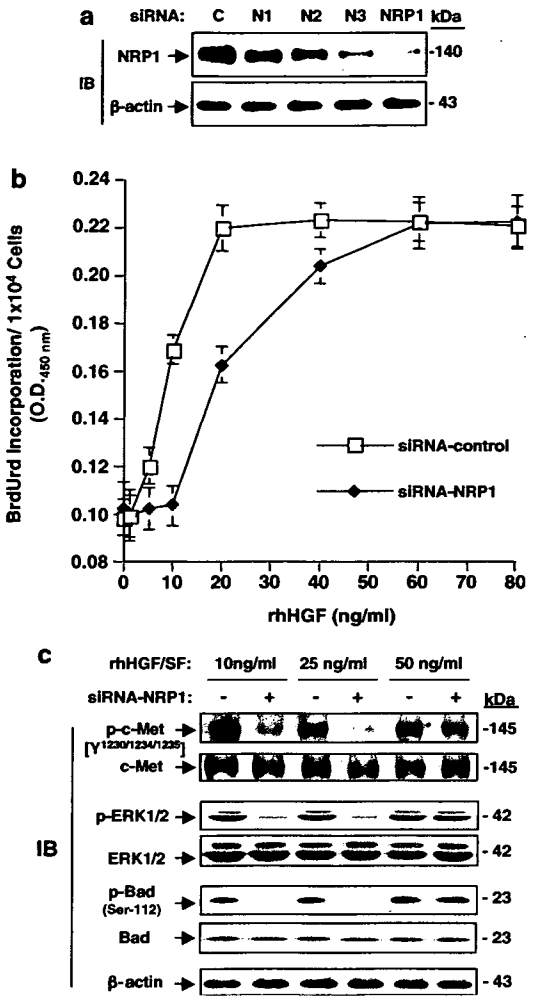

Figure 6 Inhibition of endogenous NRP1 attenuated HGF/SF stimulation of cell proliferation and HGF/SF/c-Met signaling in LNZ-308 glioma cells. (**a**) Inhibition of endogenous NRP1 by NRP1/siRNA in LNZ-308 cells detected by IB analyses. C, control siRNA. N1, N2 and N3, individual siRNAs for NRP1. NRP1, a pool of all three siRNAs of N1, N2 and N3. β-Actin was used as a loading control. (**b**) Inhibition of endogenous NRP1 in LNZ-308 cells using siRNA-attenuated rhHGF/SF stimulation of cell proliferation. Data of BrdUrd incorporation of siRNA-transfected LnZ-308 cells are shown as mean±s.d. (**c**) Inhibition of endogenous NRP1 in LNZ-308 cells using siRNA-suppressed HGF/SF stimulation of c-Met signaling detected by IB analyses. c-Met, ERK1/2 Bad and β-actin were used as loading controls. Results in (**a–c**) are representative of three independent experiments.

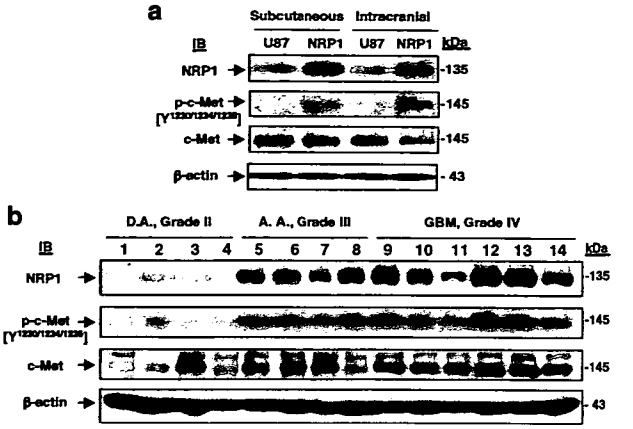

Figure 7 Upregulation of NRP1 correlates with the activation of c-Met in U87MG tumor xenografts and in high-grade human glioma specimens. (**a**) Overexpression of NRP1 in U87MG xenografts resulted in activation of c-Met in the established tumors. IB analyses of U87MG and NRP1 xenografted tumors. β-Actin was used as a loading control. (**b**) Upregulation of NRP1 expression correlates with activation of c-Met during glioma progression. IB analyses of 14 frozen primary human glioma specimens. c-Met and β-actin were used as loading controls. Results are representative of three independent experiments.

glioma specimens that upregulation of tumor cell-expressed NRP1 correlates with glioma progression and increased activation of c-Met in these clinical tumor samples. We demonstrated that overexpression of NRP1 by U87MG glioma cells enhanced tumor growth in mice through potentiating HGF/SF/c-Met activity stimulating tumor cell proliferation in mice. NRP1 potentiated the autocrine HGF/SF/c-Met signaling pathway in response to low concentrations of HGF/SF *in vitro*, and NRP1 expression is also correlated with c-Met activation in U87MG tumors that overexpress NRP1. Conversely, inhibition of tumor cell-derived HGF/SF, but not FGF-2 or VEGF, by neutralizing antibodies and of endogenous c-Met, but not Sema 3A, by specific siRNAs attenuates HGF/SF/c-Met signaling and glioma cell viability. Furthermore, suppression of endogenous NRP1 in LNZ-308 cells abolishes exogenous HGF/SF stimulation of c-Met-mediated signaling in the tumor cells at lower concentrations. Our results corroborate a recent study showing that overexpression of NRP1 in human pancreatic cancer cells resulted in constitutive activation of mitogen-activated protein kinase signaling (Wey *et al.*, 2005). A plausible mechanism of NRP1 stimulation of tumor progression in our study and the pancreatic cancer model is that NRP1 enhances endogenous signaling modulating tumor cell function independent of VEGF. Our results of NRP1 potentiation of the HGF/SF/c-Met signaling pathway in glioma cells agree with another recent study showing that that NRP1 not only interacts directly with multiple heparin-binding growth factors, such as FGF-2, FGF-4 and HGF/SF, but also potentiates stimulation of FGF-2 on endothelial cells (West *et al.*, 2005). In addition, the increased sensitivity to HGF/SF/c-Met signaling by endogenously expressed NRP1 in glioma cells is analogous to the increase in sensitivity to FGF-2 caused by the addition of a soluble NRP1 dimer to endothelial cells in the aforementioned study. Expression of NRP1 in various cell types may sensitize the cells to their microenvironments, thereby potentiating the corresponding intracellular signaling critical for cellular function.

Increased expression of NRP1 has been detected in tumor cells in clinical glioma samples, suggesting a link between NRP1 expression and glioma malignancy (Ding *et al.*, 2000). Our results further elaborate on these observations. By analysing a total of 92 primary human

glioma specimens, we show that upregulation of NRP1 in tumor cells correlates with glioma progression. In U87MG tumor xenografts, overexpression of NRP1 markedly stimulated angiogenesis at both anatomic sites (Figure 3). Significant stimulation of vessel growth by tumor cell–expressed NRP1 in our U87MG xenografts and in prostate and colon cancer models (Miao *et al.*, 2000) led to a hypothesis that tumor cell-expressed NRP1 stimulates vessel growth through a juxtacrine mechanism that forms a complex of NRP1 (in tumor cells), VEGF within the tumor microenvironment (intercellular) and VEGFR-2 (in endothelial cells), thus potentiating VEGF activity that enhances angiogenesis and tumor growth (Klagsbrun *et al.*, 2002). However, it is difficult to dissect the NRP1-stimulated juxtacrine signaling in harvested tumor tissues. Nonetheless, these data and the aforementioned studies suggest a far wider spectrum of activity of NRP1 in promoting tumor progression than is currently appreciated.

In summary, this study provides a novel mechanism that expression of NRP1 in human glioma cells promotes glioma progression through potentiating the activity of HGF/SF/c-Met autocrine pathways. Upregulation of NRP1 in tumor cells correlates with the activation of HGF/SF/c-Met pathways in both primary glioma specimens and xenograft gliomas, and inhibition of endogenous c-Met or NRP1 attenuates NRP1-enhanced HGF/SF/c-Met signaling. In addition, our data demonstrating NRP1 expression patterns in primary human glioma specimens and significant enhancement of tumor angiogenesis in glioma xenografts suggest that tumor cell-derived NRP1 stimulates vessel growth in a juxtacrine manner. These pathways appear to act in concert in promoting glioma growth and angiogenesis. Thus, our studies demonstrate a necessity for simultaneously targeting NRP1/VEGF and HGF/SF/c-Met signaling pathways in the treatment of human gliomas.

Materials and methods

Cell lines and their cultures

Human glioma cell lines U87MG, U118MG and T98G were obtained from the American Type Culture Collection (Manassas, VA, USA). Human glioma cell lines U251MG, U373MG, LNZ-308, LN229 and LN319 were from our collection. The transformed normal human astrocytes that form WHO grade III-like glioma in the murine brain (NHA/ETR) were from Dr R Pieper. Human umbilical endothelial cells (HUVEC) were from Cambrex (Rockland, ME, USA). The cells were cultured as described previously (Guo *et al.*, 2001).

siRNA transient transfection

siRNAs were synthesized by Dharmacon Inc. (Lafayette, CO, USA). The sequences of siRNA for target genes were Met, 5′-GTGCAGTATCCTCTGACAG-3′; Sema 3A, 5′-AAAGTTC ATTAGTGCCCACCT-3′ and NRP1 N1, 5′-GAGAGGTCC TGAATGTTCC-3′, N2, 5′-AAGCTCTGGGCATGGAATC AG-3′, and N3, 5′-AAAGCCCCGGGTACCTTACAT-3′; and Bad, Signal Silence Bad siRNA kit (Cell Signaling, Beverly, MA, USA). Cells were transfected with 120 nM of the indicated siRNA or a control siRNA (Invitrogen) using the Oligofectamine reagent (Invitrogen Inc., Carlsbad, CA, USA). After 24 h, siRNAs were removed and the cells were maintained in medium containing 10% FBS for an additional 48 h. The inhibition of protein expression was assessed by IB analysis.

Other methods

Reagents, antibodies, analyses of primary human glioma specimens, IHC, statistics, glioma xenograft models, immunoprecipitation (IP), IB, *in vivo* BrdUrd labeling, generation of U87MG NRP1-expressing cell lines and cell survival and proliferation assays are described in the Supplementary Information.

Acknowledgements

The work was supported by grants NIH CA102011 and RSG CSM-107144 (S-Y C), the Hillman Fellows Program for Innovative Cancer Research to S-Y C and B H, and grant NIH CA095809 to TM (in part).

References

Abounader R, Lal B, Luddy C, Koe G, Davidson B, Rosen EM *et al.* (2002). *In vivo* targeting of SF/HGF and c-met expression via U1snRNA/ribozymes inhibits glioma growth and angiogenesis and promotes apoptosis. *FASEB J* **16**: 108–110.

Abounader R, Laterra J. (2005). Scatter factor/hepatocyte growth factor in brain tumor growth and angiogenesis. *Neuro-oncol* **7**: 436–451.

Akagi M, Kawaguchi M, Liu W, McCarty MF, Takeda A, Fan F *et al.* (2003). Induction of neuropilin-1 and vascular endothelial growth factor by epidermal growth factor in human gastric cancer cells. *Br J Cancer* **88**: 796–802.

Bachelder RE, Lipscomb EA, Lin X, Wendt MA, Chadborn NH, Eickholt BJ *et al.* (2003). Competing autocrine pathways involving alternative neuropilin-1 ligands regulate chemotaxis of carcinoma cells. *Cancer Res* **63**: 5230–5233.

Bagri A, Tessier-Lavigne M. (2002). Neuropilins as Semaphorin receptors: *in vivo* functions in neuronal cell migration and axon guidance. *Adv Exp Med Biol* **515**: 13–31.

Ding H, Wu X, Roncari L, Lau N, Shannon P, Nagy A *et al.* (2000). Expression and regulation of neuropilin-1 in human astrocytomas. *Int J Cancer* **88**: 584–592.

Gagnon ML, Bielenberg DR, Gechtman Z, Miao HQ, Takashima S, Soker S *et al.* (2000). Identification of a natural soluble neuropilin-1 that binds vascular endothelial growth factor: *in vivo* expression and antitumor activity. *Proc Natl Acad Sci USA* **97**: 2573–2578.

Gao CF, Vande Woude GF. (2005). HGF/SF-Met signaling in tumor progression. *Cell Res* **15**: 49–51.

Guo P, Xu L, Pan S, Brekken RA, Yang ST, Whitaker GB *et al.* (2001). Vascular endothelial growth factor isoforms display distinct activities in promoting tumor angiogenesis at different anatomic sites. *Cancer Res* **61**: 8569–8577.

Hu B, Guo P, Fang Q, Tao HQ, Wang D, Nagane M *et al.* (2003). Angiopoietin-2 induces human glioma invasion through the activation of matrix metalloprotease-2. *Proc Natl Acad Sci USA* **100**: 8904–8909.

Klagsbrun M, Takashima S, Mamluk R. (2002). The role of neuropilin in vascular and tumor biology. *Adv Exp Med Biol* **515**: 33–48.

Laterra J, Rosen E, Nam M, Ranganathan S, Fielding K, Johnston P. (1997). Scatter factor/hepatocyte growth factor expression enhances human glioblastoma tumorigenicity and growth. *Biochem Biophys Res Commun* **235**: 743–747.

Miao HQ, Lee P, Lin H, Soker S, Klagsbrun M. (2000). Neuropilin-1 expression by tumor cells promotes tumor angiogenesis and progression. *FASEB J* **14**: 2532–2539.

Parikh AA, Fan F, Liu WB, Ahmad SA, Stoeltzing O, Reinmuth N *et al.* (2004). Neuropilin-1 in human colon cancer: expression, regulation, and role in induction of angiogenesis. *Am J Pathol* **164**: 2139–2151.

Rieger J, Wick W, Weller M. (2003). Human malignant glioma cells express semaphorins and their receptors, neuropilins and plexins. *Glia* **42**: 379–389.

West DC, Rees CG, Duchesne L, Patey SJ, Terry CJ, Turnbull JE *et al.* (2005). Interactions of multiple heparin binding growth factors with neuropilin-1 and potentiation of the activity of fibroblast growth factor-2. *J Biol Chem* **280**: 13457–13464.

Wey JS, Gray MJ, Fan F, Belcheva A, McCarty MF, Stoeltzing O *et al.* (2005). Overexpression of neuropilin-1 promotes constitutive MAPK signalling and chemoresistance in pancreatic cancer cells. *Br J Cancer* **93**: 233–241.

Supplementary Information accompanies the paper on the Oncogene website (http://www.nature.com/onc).

ELMO1 and Dock180, a Bipartite Rac1 Guanine Nucleotide Exchange Factor, Promote Human Glioma Cell Invasion

Michael J. Jarzynka,[1,2] Bo Hu,[1,3] Kwok-Min Hui,[1,2] Ifat Bar-Joseph,[1,2] Weisong Gu,[4] Takanori Hirose,[5] Lisa B. Haney,[7] Kodi S. Ravichandran,[7] Ryo Nishikawa,[6] and Shi-Yuan Cheng[1,2]

[1]Cancer Institute and Departments of [2]Pathology and [3]Medicine, University of Pittsburgh, Pittsburgh, Pennsylvania; [4]Ohio Supercomputer Center-Springfield, Springfield, Ohio; Departments of [5]Pathology and [6]Neurosurgery, Saitama Medical University, Moroyama-machi, Iruma-gun, Saitama, Japan; and [7]Beirne Carter Center for Immunology Research and Department of Microbiology, University of Virginia, Charlottesville, Virginia

Abstract

A distinct feature of malignant gliomas is the intrinsic ability of single tumor cells to disperse throughout the brain, contributing to the failure of existing therapies to alter the progression and recurrence of these deadly brain tumors. Regrettably, the mechanisms underlying the inherent invasiveness of glioma cells are poorly understood. Here, we report for the first time that engulfment and cell motility 1 (ELMO1) and dedicator of cytokinesis 1 (Dock180), a bipartite Rac1 guanine nucleotide exchange factor (GEF), are evidently linked to the invasive phenotype of glioma cells. Immunohistochemical analysis of primary human glioma specimens showed high expression levels of ELMO1 and Dock180 in actively invading tumor cells in the invasive areas, but not in the central regions of these tumors. Elevated expression of ELMO1 and Dock180 was also found in various human glioma cell lines compared with normal human astrocytes. Inhibition of endogenous ELMO1 and Dock180 expression significantly impeded glioma cell invasion *in vitro* and in brain tissue slices with a concomitant reduction in Rac1 activation. Conversely, exogenous expression of ELMO1 and Dock180 in glioma cells with low level endogenous expression increased their migratory and invasive capacity *in vitro* and in brain tissue. These data suggest that the bipartite GEF, ELMO1 and Dock180, play an important role in promoting cancer cell invasion and could be potential therapeutic targets for the treatment of diffuse malignant gliomas. [Cancer Res 2007;67(15):7203–11]

Introduction

The inherent invasive nature of malignant gliomas contributes to the high frequency of tumor recurrence and disease progression in patients afflicted with these deadly cancers. In spite of the use of multimodal therapies including surgery, radiation, and chemotherapy, the mean survival time in patients with high-grade gliomas is less than 1 year (1). It is established that the mechanisms regulating cell migration are fundamental to the invasive phenotype of gliomas (2). Although studies show that various stimuli promote glioma cell invasion, the mechanisms underlying dysregulation of cell motility during invasion of these tumor cells remain largely unknown.

Cell migration is highly regulated by spatial and temporal changes of the actin cytoskeleton essential for many physiologic and pathologic processes including cancer cell invasion. Rac1, a member of the Rho GTPase family, is a key regulator of actin cytoskeletal dynamics and relays signals from various stimuli such as growth factors, cytokines, and adhesion molecules to downstream effectors modulating cell migration and invasion (3). Importantly, Rac1 has been shown to promote glioma cell migration (4–10). The activation of Rac1 is through a GDP/GTP exchange mechanism catalyzed by the guanine nucleotide exchange factors (GEF) resulting in an active, GTP-bound state (11). The Rho GTPase GEFs are a large family of proteins that contain either a Dbl homology domain involved in nucleotide exchange (12) or a newly characterized Docker domain that facilitates GEF function (13), of which Dock180 (dedicator of cytokinesis 180) is the prototypical mammalian member.

Dock180 was first identified as a CrkII-binding protein that regulates NIH 3T3 cell morphology (14). Studies in *C. elegans* and *Drosophila* reveal that Dock180 homologues modulate various functions such as phagocytosis, cell migration, myoblast fusion, dorsal closure, and cytoskeletal organization through the activation of Rac1 (15–18). Furthermore, Dock180 stimulates phagocytosis and filopodia formation downstream of integrin receptor signaling in mammalian cells (19, 20). Importantly, Dock180 facilitates nucleotide exchange on Rac1 through its unconventional Docker GEF domain (21–23) but requires binding to engulfment and cell motility 1 (ELMO1) in achieving GDP/GTP exchange on Rac (21). In mammalian cells and in *C. elegans*, ELMO1 and its homologue, CED-12, enhance phagocytosis and cell migration by forming a complex with Dock180 (24). This bipartite GEF complex synergistically functions upstream of Rac1, promoting Rac-dependent cell migration (25). Although ELMO1 and Dock180 stimulate cell migration in normal mammalian cells, whether these molecules play a critical role in cancer cell migration and invasion has not been investigated.

In this study, we show for the first time that ELMO1 and Dock180 stimulate glioma cell migration and invasion. We detected high-level expression of ELMO1 and Dock180 in actively infiltrating glioma cells within the invasive regions along blood vessels, neuronal structures, and the corpus callosum as compared with the central tumor areas of primary human glioma specimens representing WHO grades 2 to 4. Furthermore, we found that ELMO1 and Dock180 expression is increased in human glioma cell lines compared with normal human astrocytes. Inhibition of

Note: Supplementary data for this article are available at Cancer Research Online (http://cancerres.aacrjournals.org/).

Current address for W. Gu: SuperArray Bioscience, 7320 Executive Park, Frederick, MD 21704.

Requests for reprints: Shi-Yuan Cheng, Cancer Institute and Department of Pathology, University of Pittsburgh, HCCLB, 2.26f, 5117 Centre Avenue, Pittsburgh, PA 15213. Phone: 412-623-3261; Fax: 412-623-4840; E-mail: chengs@upmc.edu or Bo Hu, Cancer Institute and Department of Medicine, University of Pittsburgh, HCCLB, 2.19f, 5117 Centre Avenue, Pittsburgh, PA 15213. Phone: 412-623-7791; Fax: 412-623-4840; E-mail: hub@upmc.edu.

doi:10.1158/0008-5472.CAN-07-0473

endogenous ELMO1 and Dock180 impeded glioma cell migration and invasion whereas forced expression of ELMO1 and Dock180 in glioma cell lines with low endogenous expression enhanced tumor cell migration and invasion *in vitro* and *ex vivo*. These data show a novel function for the bipartite GEF, ELMO1 and Dock180, in stimulating cancer cell migration and invasion.

Materials and Methods

Cell lines, antibodies, and reagents. Human LN18, LN229, U118, and U87MG glioma cells were obtained from American Type Culture Collection; U251MG and U373MG glioma cells were from our collection and their culture was previously described (26). D54MG glioma cells were from Dr. D. Bigner (Duke University, Durham, NC). SNB19 glioma cells were from Dr. Y-H. Zhou (University of California, Irvine, Irvine, CA). Immortalized normal human astrocytes and genetically modified normal human astrocytes (27) were from Dr. R. Pieper (University of California, San Francisco, San Francisco, CA). The following reagents were used in our studies: goat anti-Dock180 antibody (H-4), goat anti-Dock180 antibody (N-19), and goat anti–β-actin (I-19) antibodies (Santa Cruz Biotechnology), goat anti-ELMO1 (Ab2239, Abcam), rabbit anti-ELMO1 antibody (21), Rac1 activation assay kit (Upstate Technology), and a mouse anti-Rac1 antibody (BD PharMingen). The secondary antibodies were from Vector Laboratories or Jackson ImmunoResearch Laboratories. A 3,3′-diaminobenzidine elite kit was from DAKO; AquaBlock was from East Coast Biologics, Inc. Cell culture media and other reagents were from Hyclone, Invitrogen BRL, Sigma Chemicals, and Fisher Scientific.

Immunohistochemical analyses of primary human glioma specimens. A total of 53 human malignant glioma specimens that contain an identifiable center and border/invasive area were used and included 6 diffuse astrocytomas (grade 2), 1 oligoastrocytoma (grade 2), 5 oligodendrogliomas (grade 2), 8 anaplastic astrocytomas (grade 3), 5 anaplastic oligodendrogliomas (grade 3), 3 anaplastic oligoastrocytomas (grade 3), and 25 glioblastoma multiforme (grade 4). Additionally, four normal human brain specimens obtained at autopsy from patients without brain lesions were included as controls. Immunohistochemical analyses and scoring were done as previously described (28) with no (−), weakest (±), low (1+), medium (2+), and strong (3+) staining with a polyclonal rabbit anti-ELMO1 (1:150) and a polyclonal goat anti-Dock180 (N-19; 1:1,000) antibody.

Microdissection and protein extraction of paraffin-embedded glioma tissue. Microdissection of paraffin-embedded human glioma tissue was done as previously described (28). Briefly, the paraffin-embedded glioma specimens were sectioned at 5- and 50-μm thicknesses and mounted onto glass slides. To identify the center, border, and invasive regions within the glioma specimen, the 5-μm-thick sections were stained with H&E. Three 50-μm-thick sister sections of each sample were then deparaffinized in xylenes, rehydrated in graded ethanol, immersed in distilled water, and air-dried. To exclusively collect the center or border regions of the tissue, the targeted areas were cut microscopically under an Olympus SZ-STS stereomicroscope with a fine needle using the sister H&E-stained section as a guide. Next, total protein was extracted from the microdissected, formalin-fixed paraffin-embedded glioma tissue as previously described (28).

Immunoblotting. Thirty micrograms of total protein from various whole-cell lysates were separated by NuPAGE 10% Bis-Tris polyacrylamide gel (Invitrogen) electrophoresis under reducing conditions and transferred onto Immobilon-P transfer membranes (Millipore). The membranes were blocked, incubated with the indicated primary antibodies, and subsequently probed with peroxidase-labeled secondary antibodies. The reacted proteins were visualized by enhanced chemiluminescence reaction (Amersham Biosciences).

Inhibition of ELMO, Dock180, and Rac1 expression. Small interfering RNA (siRNA) was synthesized by Invitrogen. The target sequences of ELMO1 were 5′-GGCACUAUCCUUCGAUUAACCACAU-3′ (designated E1) and 5′-CCGAGAGGAUGAACCAGGAAGAUUU-3′ (designated E2; ref. 29). The target sequences of Rac1 were 5′-AAGGAGAUUGGUGCUGUAAAA-3′ (designated R1; ref. 6) and 5′-AACCUUUGUACGCUUUGCUCA-3′ (designated R2; refs. 6, 7). A pool containing three separate Dock180 siRNAs was from Santa Cruz Biotechnology. The glioma cells were plated at 40% to 50% confluency, were allowed to attach to the tissue culture dish for ~3 h, and transfected with 60 to 120 nmol/L of the indicated siRNA for 24 h in the presence of 10% fetal bovine serum (FBS) in DMEM using Lipofectamine 2000 following the manufacturer's instructions (Invitrogen). Mock transfection was done in parallel using the Stealth RNAi Negative Control Med GC (Invitrogen). After 24 h, the siRNA/lipid complexes were removed and the cells were maintained in complete medium for an additional 48 h or treated with the proteasome inhibitors MG132 (2 μmol/L) or ALLN (4 μmol/L) for 24 h. The inhibition of protein expression was determined by Western blot analysis.

Exogenous expression of ELMO1 and Dock180. A pCG plasmid encoding c-Myc– and His-tagged full-length human ELMO1 (from Dr. J. Skowronski, Cold Spring Harbor Laboratory, Cold Spring Harbor, NY; ref. 30) and/or a pCXN2 plasmid encoding Flag-tagged full-length human Dock180 (from Dr. M. Matsuda, Kyoto University, Kyoto, Japan) was transfected into U87MG and U251MG cells using Effectene following the manufacturer's instructions (Qiagen). Forty-eight hours posttransfection, the cells were used in *in vitro* cell migration, invasion, and *ex vivo* brain slice assays. The expression of exogenous ELMO1 and Dock180 expression was determined by Western blot analysis.

Rac1 activation assay. GTP loading of Rac1 was measured using the Rac1 Activation Assay Kit (Upstate Technology) according to the manufacturer's instructions. Briefly, cells were lysed in ice-cold magnesium lysis buffer and cleared with glutathione-agarose beads. Cell extracts were then incubated with PAK-1 PBD agarose beads, pelleted, and washed. The beads were resuspended in sample buffer and separated by 10% PAGE. GTP-bound Rac1 was detected using an anti-Rac1 antibody.

***In vitro* migration and invasion assays.** *In vitro* migration and invasion assays were done as previously described (31). Briefly, 50 μL of transiently transfected (siRNA or plasmid DNA) glioma cells (5×10^5/mL in serum-free DMEM plus 0.05% bovine serum albumin) were separately placed into the top compartment of a Boyden chamber. For migration assays, the cells were allowed to migrate through an 8-μm pore size membrane precoated with fibronectin (10 μg/mL) overnight at 37°C. For invasion assays, the cells were allowed to invade through a growth factor–reduced Matrigel–coated (0.78 mg/mL) membrane overnight at 37°C. Afterwards, the membrane was fixed and stained, nonmigrating and noninvading cells were removed, and the remaining cells were counted.

***Ex vivo* brain slice invasion assay.** The *ex vivo* brain slice assay was done as previously described with minor modifications (9, 10). Briefly, fresh sections (500-μm thickness) of mouse cerebrum from 8-week-old mice (C57/BL6, The Jackson Laboratory) were placed onto transwell membranes (0.4 μm pore size, Corning) in a six-well dish containing DMEM with 10% FBS, 100 units/mL of penicillin, and 100 μg/mL of streptomycin, allowing the surface of the brain slice to be semidry. Afterwards, green fluorescent protein (GFP)–expressing glioma cells (5×10^4 in 0.5-μL DMEM) are placed onto the putamen of both sides of each brain slice and incubated in a humidified environment at 37°C, 5% CO_2 and 95% air. After 48 h, the brain slices were gently rinsed with PBS and fixed in 4% paraformaldehyde overnight at 4°C. Lateral cell migration/invasion was assessed by direct epifluorescent examination of GFP-expressing glioma cells using a stereomicroscope (SZX12, Olympus) at ×10 magnification. Images were captured with a SPOT digital camera (Diagnostic Instrument). Depth of cell invasion into the brain slice was determined by optical sectioning using a Zeiss LSM 510 Confocal Microscope (Carl Zeiss MicroImaging, Inc.).

Statistical analysis. One-way ANOVA with Newman-Keuls posttest or paired two-way Student's *t* test was done using GraphPad Prism version 4.00 for Windows (GraphPad software). A χ^2 test was done as previously described to examine the association between immunohistochemical staining for ELMO1 and Dock180 and glioma invasion (28). $P < 0.05$ was considered statistically significant.

Results

ELMO1 and Dock180 are co-overexpressed in actively invading glioma cells of primary human glioma specimens.

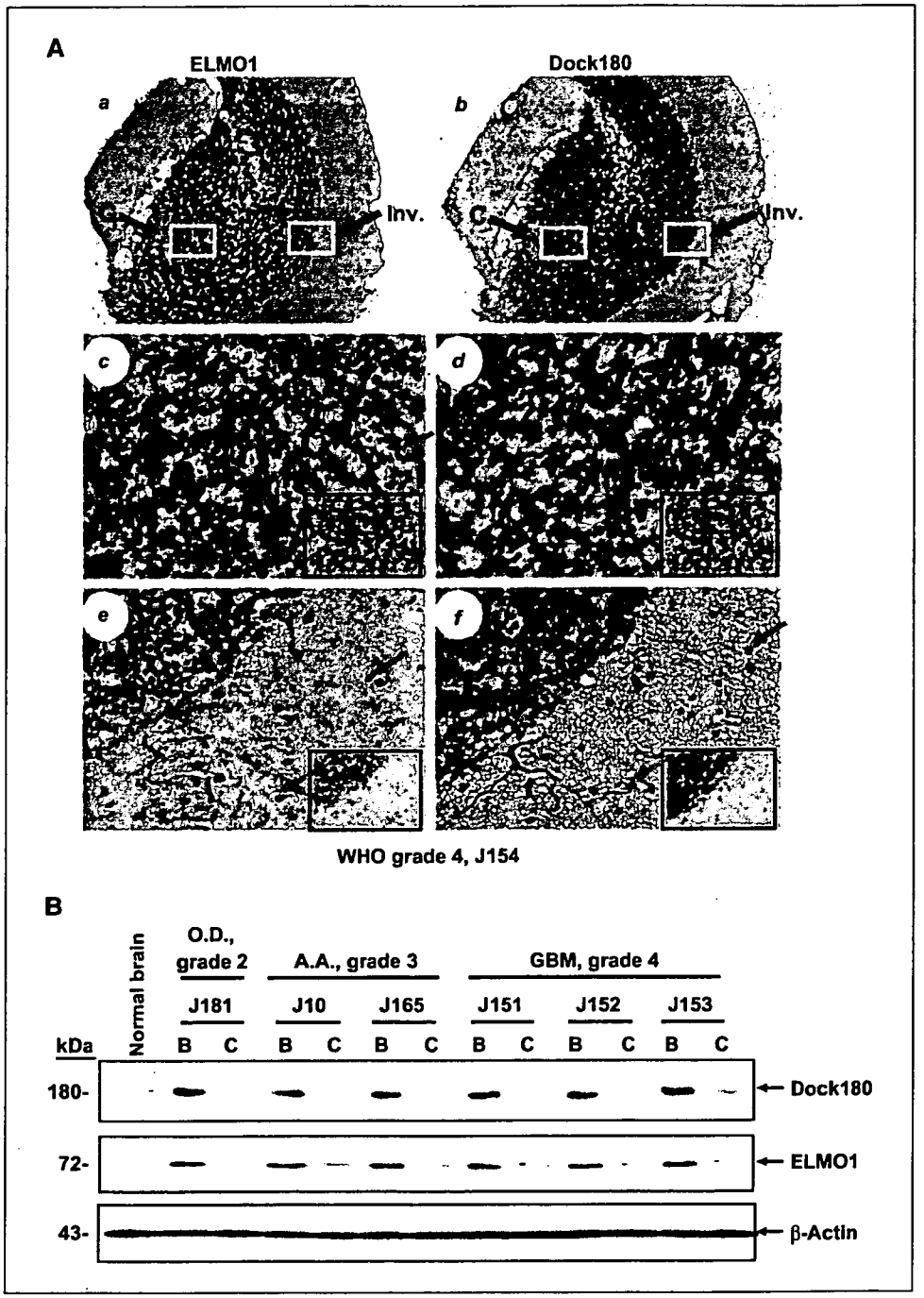

Figure 1. ELMO1 and Dock180 are co-overexpressed in invading tumor cells of primary human glioma specimens. *A*, a total of 53 individual primary tumor specimens (WHO grades 2–4) were analyzed, and representative staining of serial sections of glioblastoma multiforme (specimen J154, grade 4) tissue using a polyclonal rabbit anti-ELMO1 antibody (*a*, *c*, and *e*) and a polyclonal goat anti-Dock180 antibody (*b*, *d*, and *f*) is shown. *c* to *f*, *insets*, isotype-matched immunoglobulin G controls of the identical areas shown. *c* and *d*, enlarged central regions of the tumor mass shown in *a* and *b* (*white rectangle*). *e* and *f*, enlarged invasive areas shown in *a* and *b* (*red rectangle*). *Arrows*, positive staining for ELMO1 (*c* and *e*) and Dock180 (*f*). *Arrowheads*, unstained cells. Original magnification, ×100 (*a* and *b*); 400× (*c–f*). Representative results; immunohistochemical (*IHC*) analyses were done two additional times with similar results. *B*, immunoblot analysis of the tumor center (*C*) and invasive border (*B*) of primary glioma specimens. Total protein extracted from normal brain and microdissected glioma tissue from oligodendroglioma (*O.D.*; specimen J181, grade 2), anaplastic astrocytoma (*A.A.*; specimens J10 and J165, grade 3), and glioblastoma multiforme (*GBM*; specimens J151, J152, and J153, grade 4) was examined by immunoblotting with anti-Dock180 and anti-ELMO1 antibodies, respectively. The membranes were also probed with an anti–β-actin antibody as a loading control. Representative of three independent experiments with similar results.

The ELMO1-Dock180 complex has been shown to stimulate cell migration through the activation of Rac1 (25). Recently, we identified the up-regulation of ELMO1 gene expression in an angiopoietin-2–induced astrocytoma invasion model using global gene array followed by real-time PCR analysis,[8] signifying the potential importance of ELMO1 in promoting glioma invasion. To determine the role of ELMO1 and its binding partner Dock180 (21) in glioma cell invasion, we began by carrying out immunohistochemical analyses on a collection of primary human glioma specimens to assess whether ELMO1 and Dock180 are associated with the invasive phenotype of gliomas. We examined 53 tumors representing WHO grades 2 to 4 containing an identifiable central region and invasive areas and four normal human brain specimens (J140–J143) obtained at autopsy from patients without brain lesions as controls (28). Little to no immunoreactivity for ELMO1 and Dock180 was detected in the normal brain specimens (Supplementary Table S1; Fig. S1, *a* and *b*). Interestingly, the co-overexpression of ELMO1 and Dock180 was found in infiltrating tumor cells within the invasive areas of the glioma specimens independent of tumor grade (Fig. 1*A*, *e* and *f*; Supplementary

[8] Manuscript in preparation.

Table 1. ELMO1 and Dock180 expression correlates with glioma invasion

Immunohistochemical score	ELMO1			Dock180		
	Center	Border	Invasive	Center	Border	Invasive
3+	0	3	9	0	3	10
2+	1	12	19	1	15	22
1+	9	14	7	3	15	15
±	29	15	10	18	16	5
−	14	9	8	31	4	1
P value of correlation between positivity and tumor area*						
Border vs center		<0.01			<0.0001	
Invasive vs center		<0.0001			<0.0001	
Border vs invasive		NS			<0.05	

NOTE: The immunohistochemical staining intensity for each antibody and specimen was defined as no (−), weakest (±), low (1+), medium (2+), and strong (3+) staining as previously described (28) and is shown in Supplementary Table S1. NS, not significant ($P > 0.05$).
*Analyzed by χ^2 test for trend based on the distribution of the scores from each area.

Fig. S1, *e*, *f*, *i*, and *j*). Actively invading glioma cells observed at distant sites such as the gray matter of normal brain parenchyma, along blood vessels, neuronal structures, and the corpus callosum showed a high immunoreactivity for ELMO1 and Dock180 (data not shown). For example, in a glioblastoma multiforme (grade 4) specimen, the glioma cells invading into the adjacent brain structure (Fig. 1*A*, *e* and *f*, *arrows*) exhibited strong immunostaining by the ELMO1 and Dock180 antibodies. In contrast, Dock180 protein was not detected (Fig. 1*A*, *d*) and ELMO1 was expressed at low levels in the central core region of this same glioma tissue (Fig. 1*A*, *c*). Additionally, we failed to detect the expression of ELMO1 and Dock180 in reactive astrocytes or cells that are morphologically similar to astrocytes in invasive areas or center regions in these primary glioma specimens.

To determine whether there is a distinct link between ELMO1 and Dock180 expression and human glioma invasiveness, we did a χ^2 test for trend to examine the association between the positive staining of ELMO1 and Dock180 and each area of the glioma specimen (center, border, and invasive areas). As shown in Table 1, a significant correlation was found between the positive immunoactivities for ELMO1 ($P < 0.01$ for border versus center and $P < 0.0001$ for invasive versus center, respectively) and Dock180 ($P < 0.0001$ for both comparisons) and the invasiveness displayed by these gliomas. Of the 53 glioma samples analyzed, 67% (8 of 12) and 92% (11 of 12) WHO grade 2 specimens, 69% (11 of 16) and 75% (12 of 16) grade 3 specimens, and 84% (21 of 25) and 96% (24 of 25) grade 4 specimens showed higher expression of ELMO1 and Dock180 in the border/invasive areas versus the center region of the tumors, respectively (Supplementary Table S1).

Next, to corroborate our observation of ELMO1 and Dock180 up-regulation in invading glioma cells of the primary glioma specimens, we did immunoblotting on total protein extracted from the border/invasive regions and core area of microdissected primary glioma tissues and four normal brain specimens (28) that were used in the immunohistochemical analyses. An increase in ELMO1 and Dock180 expression was found in the border region of all six primary glioma specimens examined when compared with the center tumor area of the identical sample (Fig. 1*B*). Little to no expression of ELMO1 and Dock180 was detected in the normal brain specimens (Fig. 1*B*; Supplementary Fig. S2). These findings

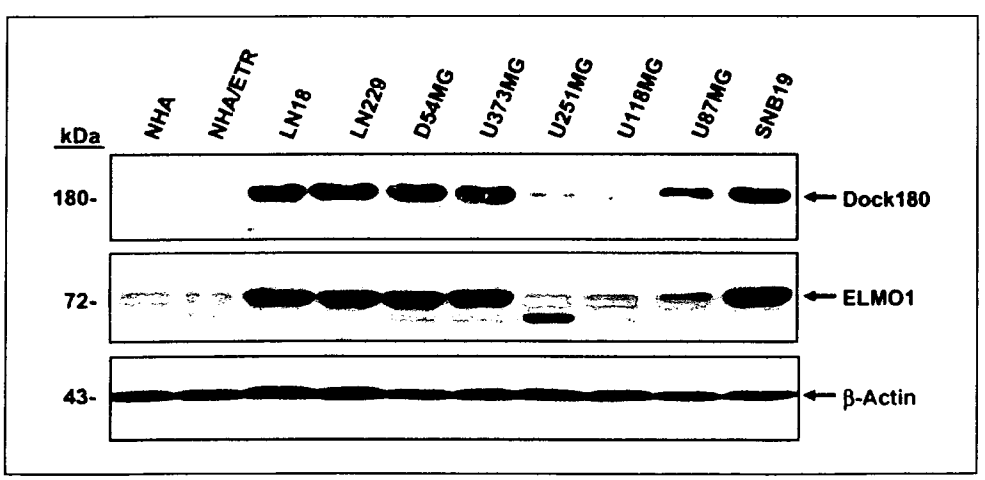

Figure 2. Endogenous expression of Dock180 and ELMO1 in various human glioma cell lines. Immunoblot analysis of normal human astrocytes (*NHA*), genetically modified normal human astrocytes (*NHA/ETR*; see Materials and Methods), and human glioma cell lysates with anti-Dock180 and anti-ELMO1 antibodies. The membranes were also probed with an anti–β-actin antibody as a loading control. Representative of three independent experiments with similar results.

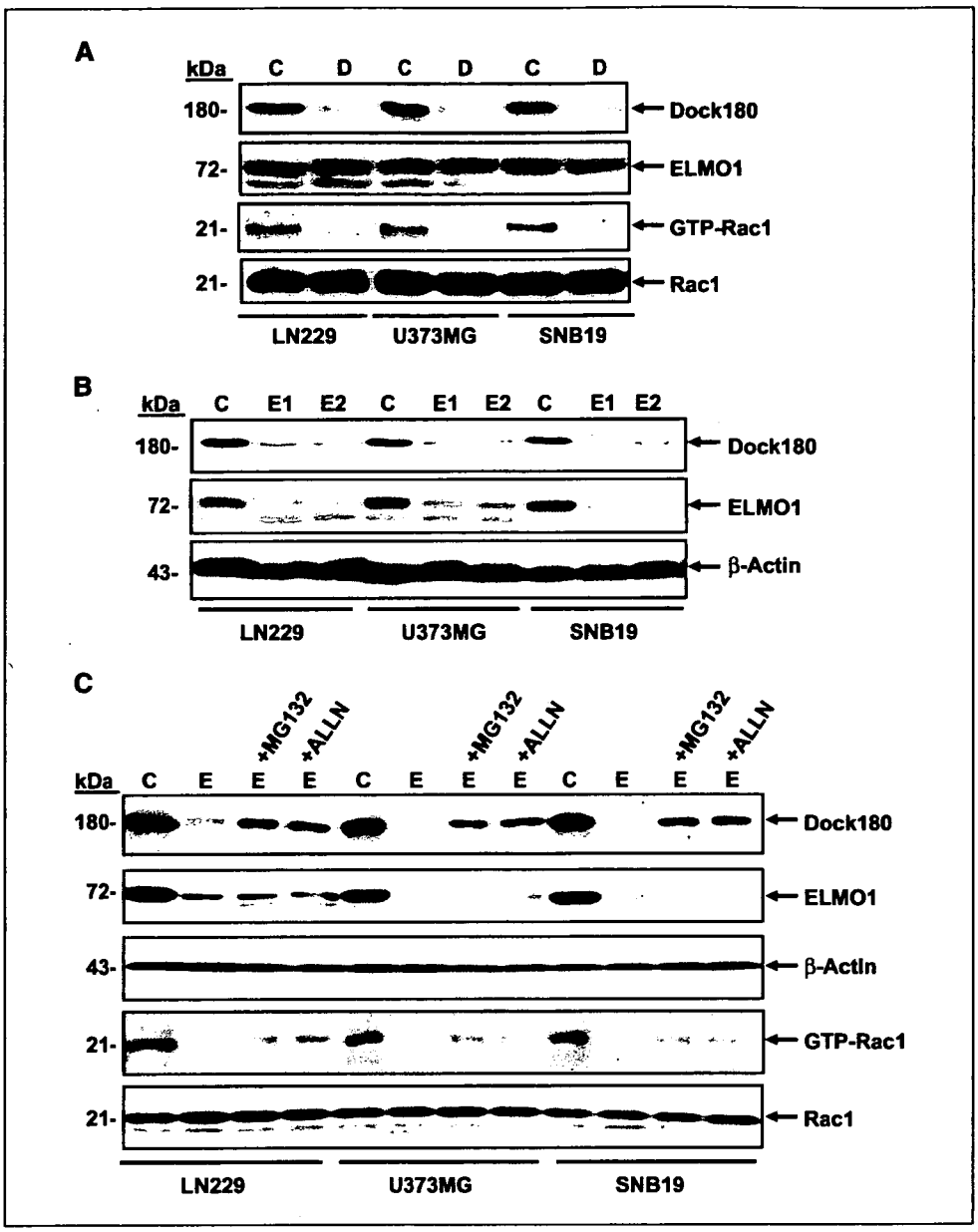

Figure 3. Suppression of endogenous ELMO1 and Dock180 inhibits GTP loading of Rac1 in glioma cells. *A* and *B*, LN229, U373MG, and SNB19 cells were transiently transfected with ELMO1 siRNA (*E1* and *E2*), Dock180 siRNA (*D*), or a control siRNA (*C*). Total cell lysates were analyzed by immunoblotting with anti-ELMO1, anti-Dock180, and anti-Rac1 antibodies and GTP loading of Rac1 using a Rac1 activation assay kit. *C*, LN229, U373MG, and SNB19 cells were transiently transfected with ELMO1 siRNA and treated with the proteasome inhibitors MG132 (2 μmol/L) or ALLN (4 μmol/L) followed by immunoblotting for ELMO1, Dock180, and Rac1 expression and GTP loading of Rac1. The membranes were also probed with an anti–β-actin antibody as a loading control. Representative of three independent experiments with similar results.

support our immunohistochemical data showing that ELMO1 and Dock180 are co-upregulated in the areas of active invasion of primary glioma specimens. Taken together, these data suggest that the expression of ELMO1 and Dock180 is consistent with the intrinsically invasive phenotype of gliomas and independent of tumor grade.

ELMO1 and Dock180 are coexpressed in human glioma cell lines. Next, we sought to determine whether ELMO1 and Dock180 play a role in glioma cell migration and invasion. We first examined the expression of ELMO1 and Dock180 in various human glioma cell lines. As shown in Fig. 2, LN18, LN229, D54MG, U373MG, and SNB19 glioma cell lines endogenously express ELMO1 and Dock180 at high levels whereas lower-level expression was found in normal human astrocytes, genetically modified normal human astrocytes (27), U251MG, U118, and U87MG glioma cell lines. In addition, the level of expression of ELMO1 correlated with the expression level of Dock180.

Inhibition of endogenously expressed ELMO1 and Dock180 suppresses Rac1 activation in glioma cells. ELMO1 and Dock180 have previously been shown to form a complex and act as a bipartite GEF thereby activating Rac1 (21). Therefore, we evaluated the significance of endogenous ELMO1 and Dock180 expression in glioma cells and determined whether inhibition of their expression by siRNA attenuates Rac1 activation. LN229, U373MG, and SNB19 glioma cells were separately transfected with ELMO1 and Dock180 siRNA. After 48 h, the glioma cells that were transiently transfected with a siRNA pool containing three target-specific sequences for Dock180 completely suppressed Dock180 expression and significantly attenuated Rac1 activation while having no effect on ELMO1 and Rac1 protein levels (Fig. 3*A*). Similarly, two different siRNAs for ELMO1 (designated E1 and E2) inhibited ELMO1 expression (Fig. 3*B*), resulting in a decrease in GTP loading of Rac1 without alteration of Rac1 protein expression (Fig. 3*C*). Interestingly, siRNA knockdown of ELMO1 also reduced the expression of Dock180 in

the glioma cells tested (Fig. 3*B* and *C*). This effect was partially blocked by the proteasome inhibitors MG132 and ALLN (Fig. 3*C*), corroborating a previous report showing that ELMO1 protects Dock180 from ubiquitylation-mediated degradation (29). These data suggest that ELMO1 and Dock180 function upstream of Rac1 and play an essential role in its activation in glioma cells.

Suppression of endogenously expressed ELMO1 and Dock180 expression inhibits glioma cell migration and invasion. Rac1, a Rho family GTPase member, induces lamellipodia formation, cell migration, and invasion in glioma cells (6). Therefore, we hypothesize that ELMO1 and Dock180 promote glioma cell migration and invasion through their effects on Rac1 activation. To test this hypothesis, we transiently transfected LN229, U373MG, and SNB19 glioma cells with ELMO1, Dock180, and Rac1 siRNA. As shown in Fig. 4*A* and Supplementary Fig. S3, suppression of ELMO1 and Dock180 expression inhibited *in vitro* glioma cell migration by 3- to 4-fold, comparable to Rac1 knockdown by siRNA (Supplementary Fig. S3). Consistent with these results, knockdown of endogenous ELMO1 and Dock180 inhibited the ability of LN229, U373MG, and SNB19 cells to invade through a growth factor–reduced Matrigel-coated membrane. Again, *in vitro* glioma cell invasion was attenuated to the same degree using ELMO1 or Dock180 siRNA as Rac1 suppression (Fig. 4*B*). These results suggest that ELMO1 and Dock180 have an essential role in promoting glioma cell migration and invasion similar to Rac1.

To test our hypothesis in a pathophysiologically relevant model, we examined whether inhibition of ELMO1 and Dock180 modulates the invasion of SNB19 and U373MG cells in a murine brain slice model (9, 10). We separately transfected GFP-expressing SNB19 and U373MG cells with control, ELMO1, or Dock180 siRNA. After 48 h, the glioma cells that were transfected with specific or control siRNAs were placed bilaterally onto the putamen of a murine brain slice and allowed to invade into the brain tissue for an additional 48 h. Afterwards, lateral migration/invasion and depth of invasion were evaluated. Inhibition of ELMO1 and Dock180 expression in both cell lines displayed less lateral migration/invasion on the brain slice compared with control siRNA–transfected or nontransfected cells (Fig. 4*C* and data not

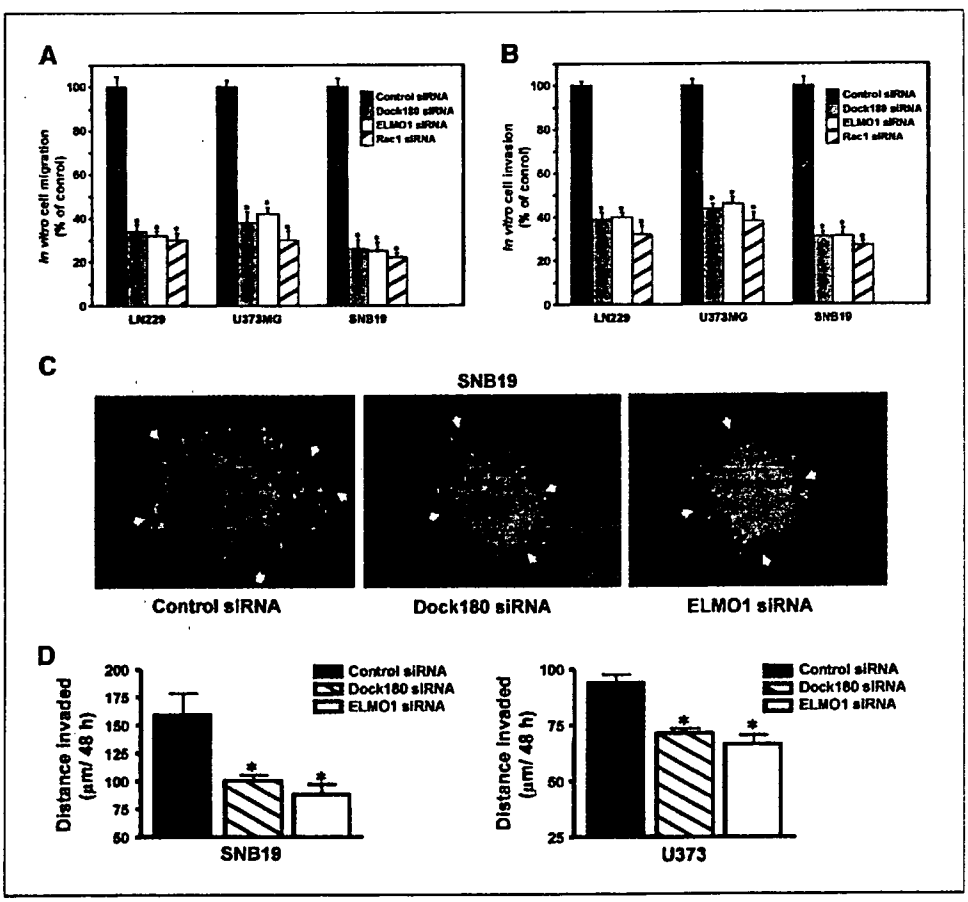

Figure 4. Suppression of endogenous ELMO1 and Dock180 inhibits glioma cell migration and invasion. *A, in vitro* cell migration assay. LN229, U373MG, and SNB19 cells were transiently transfected with the indicated siRNAs followed by cell migration assay. *B, in vitro* cell invasion assay. LN229, U373MG, and SNB19 cells were transiently transfected with the indicated siRNAs followed by an invasion assay. The migrating or invading cells were counted in 10 random high-powered fields (total magnification, ×200). Mean number of migrating or invading control cells: for migration, LN229 cells, 94.2 ± 4.6/field; U373MG cells, 73.1 ± 2.8/field; SNB19, 113.3 ± 3.8/field; and for invasion, LN229 cells, 46.7 ± 1.4/field; U373MG cells, 56.2 ± 1.9/field; SNB19, 37.2 ± 2.4/field. *Columns,* percent of control siRNA cells; *bars,* SD. *, $P < 0.05$, one-way ANOVA followed by Newman-Keuls post hoc. Three independent experiments were done in triplicate with similar results. *C,* GFP-expressing SNB19 and U373MG cells (data not shown) were transiently transfected with indicated siRNAs followed by an *ex vivo* brain slice invasion assay. Representative epifluorescent images of the GFP-expressing SNB19 cells were captured using a digital camera attached to a stereomicroscope at ×40 magnification. *D,* depth of SNB19 and U373MG cell invasion into a murine brain slice. *Columns,* mean distance (μm) invaded in 48 h from six independent experiments done in five to seven replicates per pair (control siRNA–transfected cells versus specific siRNA–transfected cells); *bars,* SE. *, $P < 0.05$, one-way ANOVA followed by Newman-Keuls post hoc. No-transfection controls for both SNB19 and U373MG cell lines were also done showing no observable effects on cell viability or the invasive ability when comparing the control siRNA–transfected and nontransfected cells (data not shown).

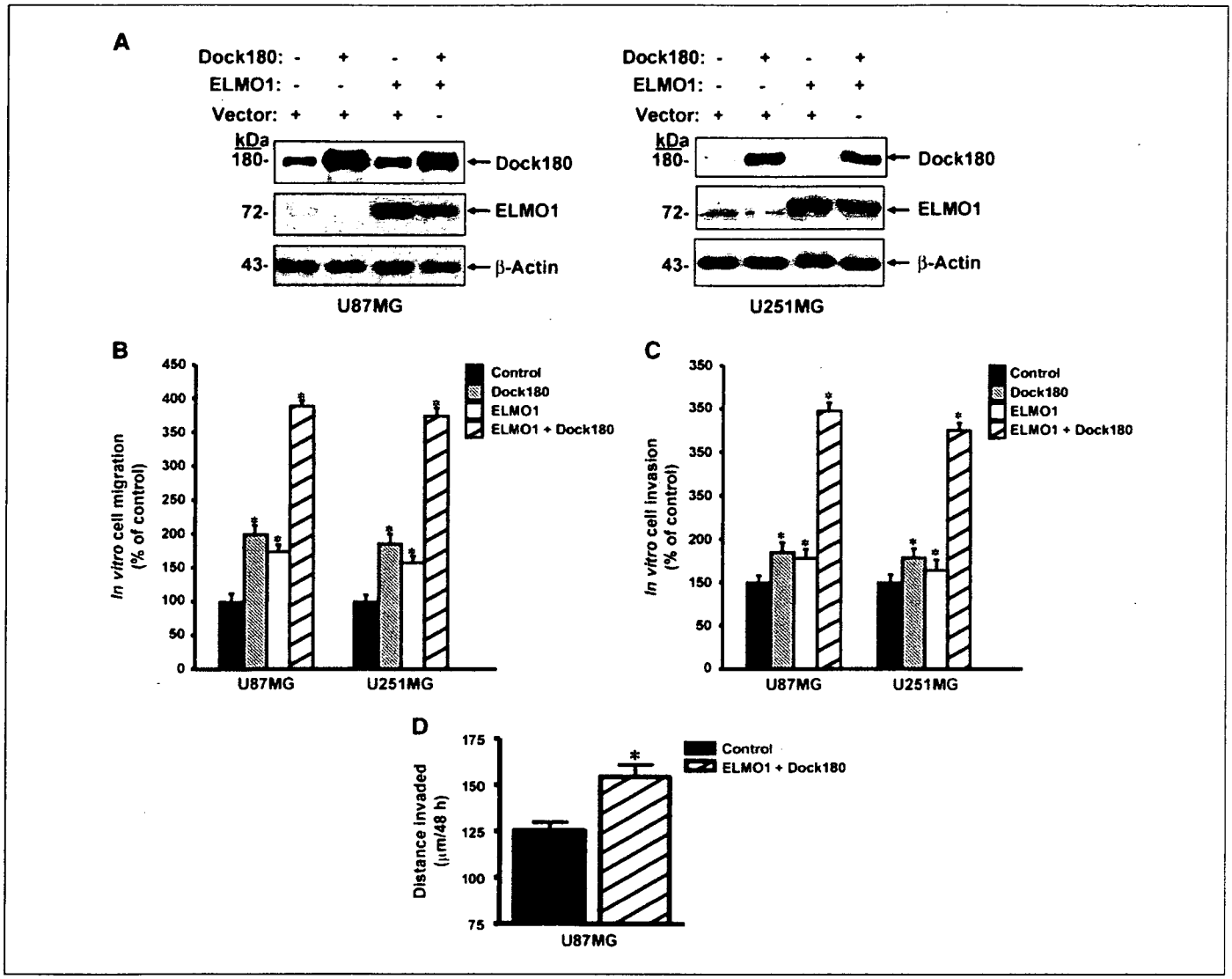

Figure 5. Exogenous expression of Dock180 and ELMO1 promotes glioma cell migration and invasion. *A*, U87MG and U251MG cells were transiently transfected with the indicated plasmids. Total cell lysates were analyzed by immunoblotting for ELMO1 and Dock180 expression. *B* and *C*, U87MG and U251MG cells were transiently transfected with the indicated plasmids followed by cell migration assay (*B*) or cell invasion assay (*C*). *D*, GFP-expressing U87MG cells were transiently transfected with the indicated plasmids and analyzed by an *ex vivo* brain slice invasion assay. *Columns*, mean distance (μm) invaded in 48 h from four independent experiments done in five to seven replicates per pair (control transfected–cells versus ELMO1- and Dock180-transfected cells); *bars*, SE. *, $P < 0.05$, paired Student's *t* test.

shown). Analysis by confocal laser scanning microscopy revealed that ELMO1 and Dock180 suppression significantly blocked the intrinsic invasiveness of the GFP-expressing SNB19 (mean ± SE, 88 ± 8.9 and 100 ± 5.2 μm/48 h, respectively) into the brain slice as compared with control siRNA–transfected or nontransfected SNB19 cells (mean ± SE, 159 ± 19 μm/48 h; Fig. 4*D* and data not shown). Similarly, glioma cell invasiveness was inhibited in the ELMO1 siRNA–treated (mean ± SE, 66 ± 4.1 μm/48 h) and Dock180 siRNA–treated (mean ± SE, 71 ± 2.2 μm/48 h) U373 cells versus the cells transfected with a control siRNA or nontransfected cells (mean ± SE, 94 ± 3.5 μm/48 h; Fig. 4*D* and data not shown). Thus, these results indicate that ELMO1 and Dock180 significantly contribute to the inherent invasive phenotype of these glioma cells *in vitro* and *ex vivo*.

Exogenous expression of ELMO1 and Dock180 stimulates glioma cell migration and invasion. In reciprocal experiments, we examined whether exogenous expression of ELMO1 and Dock180 in glioma cells that have low level endogenous expression increases glioma cell migration and invasion. First, U87MG and U251 glioma cells were transiently transfected with empty vectors, the ELMO1 and/or the Dock 180 plasmids leading to enhanced expression of these two proteins (Fig. 5*A*) and an increase in activated Rac1 (data not shown). Exogenous expression of ELMO1 and/or Dock180 in U87MG and U251MG cells increased cell migration and invasion *in vitro* with dual expression having the greatest effect of 3- to 4-fold (Fig. 5*B* and *C*).

Next, we tested whether exogenous overexpression of ELMO1 and Dock180 stimulates U87MG glioma cell invasion in the murine brain tissue. U87MG control (vector-transfected) and ELMO1/Dock180–expressing cells were separately seeded onto the murine brain slice. As shown in Fig. 5*D*, the depth of invasion into the brain slice was significantly increased in the ELMO1/Dock180–expressing

U87MG glioma cells (mean ± SE, 154 ± 6.5 μm/48 h) compared with the control transfected cells (mean ± SE, 125 ± 4.5 μm/48 h). Interestingly, the ELMO1/Dock180–expressing U87MG cells showed a similar invasion distance (mean ± SE, 154 ± 6.5 μm/48 h) as the parental SNB19 cells (mean ± SE, 159 ± 19 μm/48 h) that have high endogenous expression of ELMO1 and Dock180. Taken together, these results further confirm that ELMO1 and Dock180 are able to enhance the migration/invasion of glioma cells.

Discussion

In the present study, we provide direct functional evidence showing that ELMO1 and Dock180 play a critical role in glioma invasion. Our data suggest that preferential expression of ELMO1 and Dock180 in invading glioma cells is associated with the intrinsically invasive behavior of human gliomas. Recent studies show that localized alterations in gene and protein expression in the actively invading glioma cell population may be responsible for their more migratory and invasive phenotype compared with the glioma cells of the tumor core (5, 9, 28, 32). Our results identify a significant correlation between ELMO1 and Dock180 expression and the invasive phenotype of the gliomas, strongly corroborating this theory. Immunohistochemical analysis revealed a co-overexpression of ELMO1 and Dock180 in the infiltrating glioma cells within the border and invasive regions compared with the central core of the identical glioma specimens, independent of WHO tumor grade. We witnessed glioma cells that were strongly positive for ELMO1 and Dock180 infiltrating along blood vessels, neuronal structures, and the corpus callosum (data not shown). This display of dissemination is consistent with the unique pattern of invasion of diverse anatomic structures observed in glioma biology (2). Importantly, because all malignant gliomas have the propensity to diffusely invade normal brain areas regardless of WHO grade (33), the increased expression of ELMO1 and Dock180 in the infiltrating tumor cells may reveal an important pathologic occurrence during active glioma cell invasion.

Dock180 and ELMO1 are evolutionarily conserved proteins that are essential in multiple biological processes involving cell migration (18, 24). For example, *myoblast city*, the Dock180 homologue in *Drosophila*, is necessary for dorsal closure and cytoskeletal organization in the migrating epidermis (16). CED-5 and CED-12, the homologues of Dock180 and ELMO1, are required for phagocytosis and cell migration in *C. elegans* (18, 24). In normal mammalian cells, ELMO1 and Dock180 form a complex, function as an unconventional Rac1-GEF (21), and stimulate cell migration through Rac1 activation (25). Notably, these latter studies use forced overexpression of ELMO1 and Dock180 in human embryonic kidney 293T and murine fibroblast LR73 cells to examine the effects of both proteins. In this study, we extended these observations for the first time to human glioma models revealing a novel function of this unconventional Rac1-GEF in promoting cancer cell migration and invasion. We found that inhibition of endogenously expressed ELMO1 and Dock180 attenuates the invasive behavior of glioma cell lines concomitant with a reduction in activated Rac1. Conversely, exogenous expression of ELMO1 and Dock180 in low-level expressing glioma cells increased their capacity to migrate and invade *in vitro* and in the brain, emphasizing the importance of these molecules in the invasive process of these malignant cells.

Tumor cell invasion requires both intrinsic cellular alterations and extrinsic stimuli to trigger cell motility (34). Our study examined how endogenously or exogenously expressed ELMO1 and Dock180 affected the intrinsic aspect of glioma cell migration and invasion independent of exogenous stimuli. The modest increase in invasion of ELMO1- and Dock180-overexpressing U87MG cells into the murine brain slice suggests the need for both intrinsic and extrinsic cues for efficient glioma invasion to occur. Indeed, the lack of exogenous stimuli and the diverse genetic background of glioma cell lines that impart distinct innate characteristics may influence the varying effects of ELMO1 and Dock180 on the invasive behavior of glioma cells. Because various growth factors such as epidermal growth factor (EGF), hepatocyte growth factor/scatter factor (HGF/SF), and platelet-derived growth factor (PDGF) have been implicated in promoting glioma cell invasion (35, 36), we investigated whether these growth factors regulate ELMO1 and Dock180. EGF, HGF/SF, and PDGF did not modulate the protein expression and phosphorylation of ELMO1 and Dock180 in glioma cells. Recent studies have shown that an EGF receptor (EGFR) mutant that lacks exons 3 to 7 of its extracellular domain (EGFRvIII) and is frequently found in high grade gliomas (1) promotes glioma progression and invasion in the brain (37, 38). We have found by immunohistochemical analysis that EGFRvIII is coexpressed with ELMO1 and Dock180 in invading tumor cells within the border regions but not in the center areas of primary glioma specimens. We are currently investigating the mechanisms by which ELMO1 and Dock180 mediate EGFRvIII-promoted glioma cell invasion using *in vitro* and *in vivo* models.

Rac1 regulates spatial and temporal changes of the actin cytoskeleton by relaying signals from various stimuli such as growth factors, cytokines, and adhesion molecules to downstream effectors (3) promoting glioma cell migration (4–10). Several reports indicate that activation of Rac1 by ephrin-B3 (9), fibroblast growth factor-inducible 14 (5), neurotensin (4), and P311 (39) stimulates glioma cell motility and invasion through actin cytoskeleton reorganization. It is plausible that ELMO1/Dock180 or other Rac1-GEFs (40) are responsible for mediating these upstream signals to activate Rac1 in these glioma cell lines, and thus further investigation is warranted.

It is well established that the tumor microenvironment composed of extracellular matrix contributes to the invasive behavior of gliomas (41–43). Cell adhesion to the extracellular matrix accomplished by cell-surface receptors such as integrins is a critical first step during glioma invasion (41). Dock180 has been shown to function downstream of the $\alpha_v\beta_5$ and β_1 integrins in GD25 fibroblasts and 293T cells, respectively (19, 20). Furthermore, a ternary complex consisting of RhoG-ELMO1-Dock180 mediates integrin-induced cell spreading of HeLa cells (44). Thus, integrin signaling may constitute another important pathway in facilitating ELMO1- and Dock180-mediated glioma invasion. Within the tumor microenvironment, the stromal cells serve as an ideal source of exogenous stimuli for glioma cells by producing numerous cytokines, proteases, and other extrinsic factors that affect cancer cell motility (34). Given that ELMO1 and Dock180 are co-overexpressed in actively infiltrating glioma cells, it is also possible that these extrinsic factors within the tumor milieu modulate ELMO1 and Dock180 expression through paracrine mechanisms.

In summary, this study identifies the novel function of the unconventional GEF, ELMO1 and Dock180, in promoting glioma cell migration and invasion. Co-overexpression of ELMO1 and Dock180 in actively infiltrating glioma cells illustrates a significant association between these Rac1 regulatory proteins and the invasive phenotype of diffuse gliomas. Because aberrant activation

of cell motility pathways may underlie cancer cell invasion, understanding the mechanisms by which ELMO1 and Dock180 mediate glioma cell invasion could establish these proteins as potential targets for effective therapies in the treatment of these deadly tumors.

Acknowledgments

Received 2/5/2007; revised 4/8/2007; accepted 5/21/2007.

Grant support: NIH grant CA102011, American Cancer Society grant RSG CSM-107144 (S.Y. Cheng), and the Hillman Fellows Program (S-Y. Cheng and B. Hu).

The costs of publication of this article were defrayed in part by the payment of page charges. This article must therefore be hereby marked *advertisement* in accordance with 18 U.S.C. Section 1734 solely to indicate this fact.

We thank G. Wang for assistance in the use of laser confocal microscope, M. Nakada for help with the *ex vivo* brain slice invasion assay, J. Skowronski for the human ELMO1 plasmid and M. Matsuda for the human Dock180 plasmid, D. Bigner for the D54MG cells, Y-H. Zhou for the SNB19 cells, and R. Pieper for the immortalized normal human astrocytes and genetically modified normal human astrocytes.

References

1. Maher EA, Furnari FB, Bachoo RM, et al. Malignant glioma: genetics and biology of a grave matter. Genes Dev 2001;15:1311–33.
2. Giese A, Bjerkvig R, Berens ME, Westphal M. Cost of migration: invasion of malignant gliomas and implications for treatment. J Clin Oncol 2003;21:1624–36.
3. Etienne-Manneville S, Hall A. Rho GTPases in cell biology. Nature 2002;420:629–35.
4. Servotte S, Camby I, Debeir O, et al. The in vitro influences of neurotensin on the motility characteristics of human U373 glioblastoma cells. Neuropathol Appl Neurobiol 2006;32:575–84.
5. Tran NL, McDonough WS, Savitch BA, et al. Increased fibroblast growth factor-inducible 14 expression levels promote glioma cell invasion via Rac1 and nuclear factor-κB and correlate with poor patient outcome. Cancer Res 2006;66:9535–42.
6. Chan AY, Coniglio SJ, Chuang YY, et al. Roles of the Rac1 and Rac3 GTPases in human tumor cell invasion. Oncogene 2005;24:7821–9.
7. Salhia B, Rutten F, Nakada M, et al. Inhibition of Rho-kinase affects astrocytoma morphology, motility, and invasion through activation of Rac1. Cancer Res 2005;65:8792–800.
8. Murai T, Miyazaki Y, Nishinakamura H, et al. Engagement of CD44 promotes Rac activation and CD44 cleavage during tumor cell migration. J Biol Chem 2004;279:4541–50.
9. Nakada M, Drake KL, Nakada S, Niska JA, Berens ME. Ephrin-B3 ligand promotes glioma invasion through activation of Rac1. Cancer Res 2006;66:8492–500.
10. Valster A, Tran NL, Nakada M, et al. Cell migration and invasion assays. Methods 2005;37:208–15.
11. Raftopoulou M, Hall A. Cell migration: Rho GTPases lead the way. Dev Biol 2004;265:23–32.
12. Hall A. Rho GTPases and the control of cell behaviour. Biochem Soc Trans 2005;33:891–5.
13. Meller N, Merlot S, Guda C. CZH proteins: a new family of Rho-GEFs. J Cell Sci 2005;118:4937–46.
14. Hasegawa H, Kiyokawa E, Tanaka S, et al. DOCK180, a major CRK-binding protein, alters cell morphology upon translocation to the cell membrane. Mol Cell Biol 1996;16:1770–6.
15. Kiyokawa E, Hashimoto Y, Kobayashi S, et al. Activation of Rac1 by a Crk SH3-binding protein, DOCK180. Genes Dev 1998;12:3331–6.
16. Erickson MR, Galletta BJ, Abmayr SM. *Drosophila* myoblast city encodes a conserved protein that is essential for myoblast fusion, dorsal closure, and cytoskeletal organization. J Cell Biol 1997;138:589–603.
17. Nolan KM, Barrett K, Lu Y, et al. Myoblast city, the *Drosophila* homolog of DOCK180/CED-5, is required in a Rac signaling pathway utilized for multiple developmental processes. Genes Dev 1998;12:3337–42.
18. Wu YC, Horvitz HR. *C. elegans* phagocytosis and cell-migration protein CED-5 is similar to human DOCK180. Nature 1998;392:501–4.
19. Albert ML, Kim JI, Birge RB. αvβ5 integrin recruits the CrkII-Dock180-1 complex for phagocytosis of apoptotic cells. Nat Cell Biol 2000;2:899–905.
20. Gustavsson A, Yuan M, Fallman M. Temporal dissection of β1-integrin signaling indicates a role for p130Cas-Crk in filopodia formation. J Biol Chem 2004;279:22893–901.
21. Brugnera E, Haney L, Grimsley C, et al. Unconventional Rac-GEF activity is mediated through the Dock180-ELMO complex. Nat Cell Biol 2002;4:574–82.
22. Cote JF, Vuori K. Identification of an evolutionarily conserved superfamily of DOCK180-related proteins with guanine nucleotide exchange activity. J Cell Sci 2002;115:4901–13.
23. Cote JF, Vuori K. *In vitro* guanine nucleotide exchange activity of DHR-2/DOCKER/CZH2 domains. Methods Enzymol 2006;406:41–57.
24. Gumienny TL, Brugnera E, Tosello-Trampont AC, et al. CED-12/ELMO, a novel member of the CrkII/Dock180/Rac pathway, is required for phagocytosis and cell migration. Cell 2001;107:27–41.
25. Grimsley CM, Kinchen JM, Tosello-Trampont AC, et al. Dock180 and ELMO1 proteins cooperate to promote evolutionarily conserved Rac-dependent cell migration. J Biol Chem 2004;279:6087–97.
26. Furnari FB, Lin H, Huang HS, Cavenee WK. Growth suppression of glioma cells by PTEN requires a functional phosphatase catalytic domain. Proc Natl Acad Sci U S A 1997;94:12479–84.
27. Sonoda Y, Ozawa T, Hirose Y, et al. Formation of intracranial tumors by genetically modified human astrocytes defines four pathways critical in the development of human anaplastic astrocytoma. Cancer Res 2001;61:4956–60.
28. Guo P, Imanishi Y, Cackowski FC, et al. Up-regulation of angiopoietin-2, matrix metalloprotease-2, membrane type 1 metalloprotease, and laminin 5γ2 correlates with the invasiveness of human glioma. Am J Pathol 2005;166:877–90.
29. Makino Y, Tsuda M, Ichihara S, et al. Elmo1 inhibits ubiquitylation of Dock180. J Cell Sci 2006;119:923–32.
30. Janardhan A, Swigut T, Hill B, Myers MP, Skowronski J. HIV-1 Nef binds the DOCK2-1 complex to activate rac and inhibit lymphocyte chemotaxis. PLoS Biol 2004;2:E6.
31. Hu B, Guo P, Fang Q, et al. Angiopoietin-2 induces human glioma invasion through the activation of matrix metalloprotease-2. Proc Natl Acad Sci U S A 2003;100:8904–9.
32. Demuth T, Berens ME. Molecular mechanisms of glioma cell migration and invasion. J Neurooncol 2004;70:217–28.
33. Kleihues P, Cavenee WK; International Agency for Research on Cancer. Pathology and genetics of tumours of the nervous system. Lyon: IARC Press; 2000. p. 314.
34. Sahai E. Mechanisms of cancer cell invasion. Curr Opin Genet Dev 2005;15:87–96.
35. Christofori G. New signals from the invasive front. Nature 2006;441:444–50.
36. Hamel W, Westphal M. Growth factors in gliomas revisited. Acta Neurochir (Wien) 2000;142:113–37; discussion 37–8.
37. Bachoo RM, Maher EA, Ligon KL, et al. Epidermal growth factor receptor and Ink4a/Arf: convergent mechanisms governing terminal differentiation and transformation along the neural stem cell to astrocyte axis. Cancer Cell 2002;1:269–77.
38. Wei Q, Clarke L, Scheidenhelm DK, et al. High-grade glioma formation results from postnatal Pten loss or mutant epidermal growth factor receptor expression in a transgenic mouse glioma model. Cancer Res 2006;66:7429–37.
39. McDonough WS, Tran NL, Berens ME. Regulation of glioma cell migration by serine-phosphorylated P311. Neoplasia 2005;7:862–72.
40. Rossman KL, Der CJ, Sondek J. GEF means go: turning on RHO GTPases with guanine nucleotide-exchange factors. Nat Rev Mol Cell Biol 2005;6:167–80.
41. Bellail AC, Hunter SB, Brat DJ, Tan C, Van Meir EG. Microregional extracellular matrix heterogeneity in brain modulates glioma cell invasion. Int J Biochem Cell Biol 2004;36:1046–69.
42. Giese A, Rief M, Loo M, Berens M. Determinants of human astrocytoma migration. Cancer Res 1994;54:3897–904.
43. Rao JS. Molecular mechanisms of glioma invasiveness: the role of proteases. Nat Rev Cancer 2003;3:489–501.
44. Katoh H, Negishi M. RhoG activates Rac1 by direct interaction with the Dock180-binding protein Elmo. Nature 2003;424:461–4.

4. グリオーマにおけるテモゾロミド療法

埼玉医科大学国際医療センター包括的がんセンター脳・脊髄腫瘍科教授　西川　亮

key words　glioma, chemotherapy, temozolomide, myelodysplastic syndrome, O^6-methylguanine-DNA transferase

要　旨

テモゾロミドは膠芽腫以外にもanaplastic gliomaやlow-grade gliomaにおける効果が次々と示されている．欧米においては新しい臨床試験が続々と始まっていて今後の動向が注目される．また種々の薬剤との併用の効果も試されている．耐性克服の観点からニトロソウレア製剤との併用の効果が模索されたが，BCNUとCCNUにおいて相反する結果が報告された．新しい投与スケジュールとしては three weeks on and one week off法や one-week on/one-week off法が提唱され，優れた治療効果が示されている．一方で二次癌，特に骨髄異形成症候群や白血病の報告が散見されるようになり，長期投与に対する危惧も生じている．

動　向

テモゾロミドは膠芽腫に対して人類が初めて手にした有効な化学療法薬である．放射線照射単独とテモゾロミド併用放射線照射を比較する第3相試験において有意の生存期間延長効果が得られた．近年は，膠芽腫以外の腫瘍への応用の可能性も探られている．

またテモゾロミドは副作用が軽度であることも利点であり，他の薬剤との併用や，テモゾロミド自身のdose intensityを高める試みが報告されてきている．テモゾロミドに対する感受性の一部がO^6-methylguanine-DNA methyltransferaseに依存していることが知られ，感受性を向上させるために他のニトロソウレア製剤と併用する試みや，テモゾロミド低用量持続投与の試みも行われている．

一方で，テモゾロミドはアルキル化剤であることから二次癌の発生が危惧される．実際ここ2～3年，骨髄異形成症候群や白血病の報告が散見されるようになってきた．長期間にわたってテモゾロミドを投与する場合には，二次癌発生の危険について充分に認識する必要がある．

テモゾロミドは膠芽腫において人類が初めて手にした有効な化学療法薬である．膠芽腫におけるテモゾロミドの位置づけについては複数の総説が書かれているので[1]，本稿ではA．膠芽腫以外のグリオーマにおけるテモゾロミド，B．ニトロソウレアとの併用療法，C．新しい投与スケジュール，D．二次癌の報告について概説する．

A. 膠芽腫以外のグリオーマにおけるテモゾロミド

1. 退形成性乏突起膠腫

退形成性乏突起膠腫が塩酸プロカルバジン＋CCNU＋ビンクリスチンによる化学療法（PCV療法）に高い感受性を示すこと，さらにその感受性が染色体1pと19qの欠失の有無と相関していることは20世紀末の大きなトピックであった[2]．しかしEuropean Organisation for Research and Treatment of Cancer(EORTC)とRadiation Therapy Oncology Group（RTOG）がそれぞれ行った第III相試験の結果，予想に反して，放射線照射にPCV療法を加えることによる生存期間延長効果はいずれの試験によっても否定された[3,4]．無増悪生存期間においてはPCV療法を加えた群が有意に延長していたので，PCV療法に再発を遅らせる効果があることは認められた．一方で，PCV療法群においてはgrade 3/4の有害事象が65%の症例でみられたことから，PCV療法が初回から行うべき治療であるかどうかは慎重な検討を要すると考えられた．

これに対してテモゾロミドは，第II相試験で再発乏突起膠腫に対しては約50%の奏効率が報告され[5]，またgrade 3/4の有害事象の頻度がたかだか10%であることから[6]，PCV療法にかわる化学療法として最も有望視されている．退形成性乏突起膠腫の初期治療におけるテモゾロミドの有効性については，放射線照射との併用効果を検討する第III相試験がEORTC，RTOGその他のグループ共同のintergroup studyとして準備中である．

2. 退形成性星細胞腫

退形成性星細胞腫は膠芽腫よりも化学療法に対する感受性が優れていると考えられている．したがってより感受性が劣っていると考えられる膠芽腫においてテモゾロミドの有意の生存期間延長効果が示されたことから[7]，退形成性星細胞腫においては当然テモゾロミドが有効であると推測されているが，これはまだ確固たるエビデンスが確立していない．

過去Levinらはランダム化比較試験において，放射線照射と併用する化学療法としてのBCNUとPCV療法を比較した[8]．退形成性星細胞腫においてPCV療法群で有意の生存期間延長効果が認められた．一方，英国のMedical Research Councilによるランダム化比較試験においてはPCV療法併用群と放射線照射単独群との間に生存期間の差は認められなかった[9]．したがって現時点における退形成星細胞腫の標準治療は放射線照射にPCV療法を併用するともいえるし，あるいは化学療法を併用しない放射線照射単独であるともいえる．

再発退形成性星細胞腫に対してテモゾロミドを投与した成績では，腫瘍縮小率30～40%，6カ月無増悪生存率40～50%であった[6,10]．現在RTOGによって退形成星細胞腫を対象とし，初期治療として放射線照射にBCNUを併用する群とテモゾロミドを併用する群を比較する第III相試験が進行中である．

3. Low grade glioma

星細胞腫あるいは乏突起膠腫の149例に対してテモゾロミドを投与した成績が報告されている[11]．CRはなくPR 22/149(15%)，MR 57/149 (38%)，SD 55/149 (37%)，PD 14/149 (10%)で，最大効果に達するまでの期間の中央値は12カ月と記載されている．無増悪生存期間中央値は28カ月である．画像上の腫瘍縮小効果がみられなかった症例においても痙攣の頻度が減少したりhealth-related quality of lifeが改善するなどの臨床的効果が認められた．この結果は次のステップとして，テモゾロミド単独治療と放射線照射と

の比較試験を行う根拠となり得るものと考えられ，第III相試験がEORTCによって進行中である．

染色体1pと19qの欠失の有無とテモゾロミドの効果を関係づけた興味深い報告がある[12]．107例のlow-grade gliomaの腫瘍径の変化を解析した結果，(1) 無治療の段階では1p/19qの欠失のある腫瘍の方が生育速度が遅いこと，(2) テモゾロミド投与によって92%の症例において腫瘍径がいったんは小さくなる．そして再び腫瘍が増大を始めるまでの時間が1p/19qの欠失のある腫瘍において長いこと，(3) 腫瘍径はstableであるが，充分な期間にわたって（12～30 cycles）投与されたと判断されテモゾロミドが中止された症例では，中央値200日後に腫瘍は再び増大を始めた．これらの結果はlow-grade gliomaにおいて1p/19qの欠失のある腫瘍とない腫瘍は生物学的に別個の腫瘍として扱うべきであることを示しているとともに，腫瘍がPDにならない限りはテモゾロミド投与を継続すべきではないかということを示唆している．後述するテモゾロミドによる二次癌の問題とも関係する今後の課題である．

B. ニトロソウレアとの併用

O^6-methylguanine-DNA methyltransferase (MGMT) は腫瘍のニトロソウレア製剤に対する感受性に関与していることが知られている．膠芽腫に対してテモゾロミドを用いた初期治療においてもMGMTの活性が予後予測因子であることが示されている[13]．BCNUやCCNU等とテモゾロミドを併用すると一方の投与によってMGMTが消費され，結果として感受性が改善されるという仮説がある．この仮説に従えばBCNUあるいはCCNUとテモゾロミドを併用することによって，MGMTの活性が保たれている（promotorがunmethylated）腫瘍，すなわちニトロソウレア製剤に感受性の低い群の治療成績が改善するはずである．ドイツのグループは膠芽腫初期治療において放射線照射との併用下に，CCNUをday 1に，テモゾロミドをday 2～6に投与する方法を評価した[14]．しかし，放射線照射＋テモゾロミド治療に比べて生存期間が改善したのはMGMT promotor methylatedの群においてのみであった（表1）．一方BCNUとの併用においてはMGMT promotor unmethylatedの群において生存期間の延長が認められたという報告があり[15]，今後の課題である．

表1 MGMT promotor methylationの有無による無増悪再生存期間（カ月）

	methylated	unmethylated
CCNU＋TMZ[14]	19	6
BCNU＋TMZ[15]	10.7	9.4
TMZ[16]	10.3	5.9

膠芽腫の初期治療として放射線照射にそれぞれの化学療法を併用した成績．CCNU＋TMZの場合はTMZ単独に比べてMGMT promotor methylatedの群において生存期間が延長している．
一方BCNU＋TMZの場合，TMZ単独に比べて無増悪生存期間が延長しているのはMGMT promotor methylationのない群である．

C. 新しい投与スケジュール

テモゾロミドの利点の一つは副作用が少ないことである．標準的な投与法である200mg/m^{2}を4週間毎に5日間投与する方法において，CTCAE grade 3以上の有害事象を認める頻度はリンパ球数減少を除いてたかだか10%である[6]．したがって用量を増やす投与法が試みられている．

一つは75mg/m^{2}のテモゾロミドを3週間投与し1週間休薬するthree weeks on and one week offとよばれる方法である[16]．少量を持続的に投与することによってMGMTを枯渇化させようというコンセプトであるが，6カ月無増悪生存率